AD-A126 721 AN EXPERIMENTAL STUDY OF NUCLEATE POOL BOILING HEAT TRANSFER FROM A GEWA-T FINNED SURFACE IN FREON-113(U) NAVAL POSTGRADUATE SCHOOL MONTEREY CA B G HERNANDEZ DEC 82 F/G 20/13 NL

UNCLASSIFIED

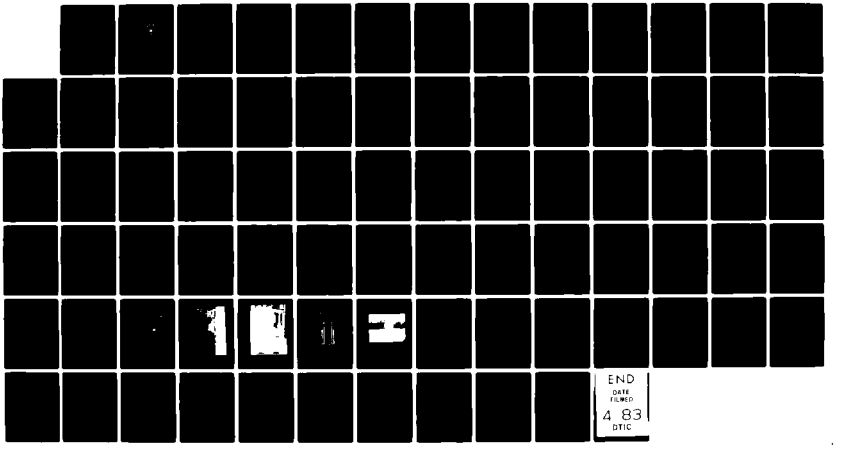

END
DATE FILMED
4 83
DTIC

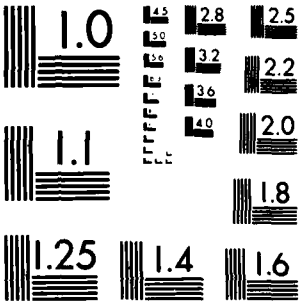

MICROCOPY RESOLUTION TEST CHART
NATIONAL BUREAU OF STANDARDS 1964 A

NAVAL POSTGRADUATE SCHOOL
Monterey, California

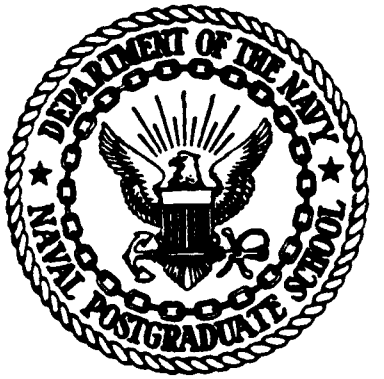

THESIS

A

AN EXPERIMENTAL STUDY OF NUCLEATE POOL BOILING HEAT TRANSFER FROM A GEWA-T FINNED SURFACE IN FREON-113

by

Bonifacio G. Hernandez, Jr.

December 1982

Thesis Advisor: P. J. Marto

UNCLASSIFIED

SECURITY CLASSIFICATION OF THIS PAGE (When Data Entered)

REPORT DOCUMENTATION PAGE		READ INSTRUCTIONS BEFORE COMPLETING FORM
1. REPORT NUMBER	2. GOVT ACCESSION NO. A126721	3. RECIPIENT'S CATALOG NUMBER
4. TITLE (and Subtitle) An Experimental Study of Nucleate Pool Boiling Heat Transfer from a Gewa-T Finned Surface in Freon-113		5. TYPE OF REPORT & PERIOD COVERED Master's Thesis; December 1982
		6. PERFORMING ORG. REPORT NUMBER
7. AUTHOR(s) Bonifacio G. Hernandez, Jr.		8. CONTRACT OR GRANT NUMBER(s)
9. PERFORMING ORGANIZATION NAME AND ADDRESS Naval Postgraduate School Monterey, California 93940		10. PROGRAM ELEMENT, PROJECT, TASK AREA & WORK UNIT NUMBERS
11. CONTROLLING OFFICE NAME AND ADDRESS Naval Postgraduate School Monterey, California 93940		12. REPORT DATE December 1982
		13. NUMBER OF PAGES 77
14. MONITORING AGENCY NAME & ADDRESS(if different from Controlling Office)		15. SECURITY CLASS. (of this report) Unclassified
		15a. DECLASSIFICATION/DOWNGRADING SCHEDULE

16. DISTRIBUTION STATEMENT (of this Report)

Approved for public release; distribution unlimited.

17. DISTRIBUTION STATEMENT (of the abstract entered in Block 20, if different from Report)

18. SUPPLEMENTARY NOTES

19. KEY WORDS (Continue on reverse side if necessary and identify by block number)

Nucleate Pool Boiling

Gewa-T Finned Surface

20. ABSTRACT (Continue on reverse side if necessary and identify by block number)

A variety of experimental tests were made with a Gewa-T finned surface in Freon-113 to assist in understanding the physical mechanisms which occur during nucleate pool boiling from this type of surface.

The influence of the channels between neighboring T-shaped fins was examined with the use of four aluminum shrouds which had top and bottom windows of various apertures, and which were

DD FORM 1 JAN 73 1473 EDITION OF 1 NOV 65 IS OBSOLETE S/N 0102-014-6601

UNCLASSIFIED

SECURITY CLASSIFICATION OF THIS PAGE (When Data Entered)

#20 - ABSTRACT - (CONTINUED)

fitted tightly over the Gewa-T surface. The influence of the fins was examined by progressively machining away the fin height to arrive at a smooth cylindrical surface.

The application of the shrouds increased the heat transfer coefficient at low heat fluxes by as much as 153 percent, but decreased the heat transfer coefficient at high heat fluxes when compared to the unshrouded surface. The addition of the "T-caps" to straight fins produced the most significant improvement in heat transfer performance when compared to a smooth tube. Based upon these results, it appears that the heat transfer performance of the Gewa-T surface is mainly influenced by the effect of the channels created by neighboring T-shaped fins.

Approved for public release; distribution unlimited.

An Experimental Study of Nucleate Pool Boiling Heat Transfer from a Gewa-T Finned Surface in Freon-113

by

Bonifacio G. Hernandez, Jr.
Lieutenant, United States Navy
B.S., Columbia University, 1975

Submitted in partial fulfillment of the requirements for the degree of

MASTER OF SCIENCE IN MECHANICAL ENGINEERING

from the

NAVAL POSTGRADUATE SCHOOL

December 1982

Author: B. G. Hernandez, Jr.

Approved by: P. J. Marto
Thesis Advisor

M. R. Morgan
Second Reader

P. J. Marto
Chairman, Department of Mechanical Engineering

William M. Tolles
Dean of Science and Engineering

ABSTRACT

A variety of experimental tests were made with a Gewa-T finned surface in Freon-113 to assist in understanding the physical mechanisms which occur during nucleate pool boiling from this type of surface.

The influence of the channels between neighboring T-shaped fins was examined with the use of four aluminum shrouds which had top and bottom windows of various apertures, and which were fitted tightly over the Gewa-T surface. The influence of the fins was examined by progressively machining away the fin height to arrive at a smooth cylindrical surface.

The application of the shrouds increased the heat transfer coefficient at low heat fluxes by as much as 153 percent, but decreased the heat transfer coefficient at high heat fluxes when compared to the unshrouded surface. The addition of the "T-caps" to straight fins produced the most significant improvement in heat transfer performance when compared to a smooth tube. Based upon these results, it appears that the heat transfer performance of the Gewa-T surface is mainly influenced by the effect of the channels created by neighboring T-shaped fins.

TABLE OF CONTENTS

LIST OF FIGURES

ACKNOWLEDGMENTS

The completion of this investigation is a reflection of the faithful support and encouragement which the author received from his family, friends, and the faculty of the Naval Postgraduate School. The author is sincerely grateful for the assistance rendered willingly by Professors William Culbreth, Paul Pucci, and Joseph Sladky.

The author offers his sincere appreciation to Professor Paul Marto for his untiring patience, and his willingness to provide invaluable assistance and attention to this work at any given time.

Finally, thank you Almighty Father.

I. INTRODUCTION

A. BACKGROUND

Nucleate pool boiling is characterized by bubble formation on a heated surface immersed in a liquid pool. The bubble nucleation and the subsequent bubble separation from the surface induce fluid motion, or mixing, near the surface which enhances heat transfer from the heated surface to the liquid. Techniques to enhance boiling heat transfer are being vigorously pursued as the costs of labor, material, and energy continue to escalate. The techniques which have received the greatest attention are those which promote nucleation as a result of surface enhancement.

The purpose of surface enhancement is to provide stable nucleation sites at a lower wall superheat than that which is required for boiling from the natural cavities of the surface, and thereby produce an improvement in the heat transfer performance over that of the unenhanced surface. Improving the heat transfer performance in this manner yields a corresponding increase in the heat transfer coefficient due to the lower wall superheat required for boiling. Therefore, the enhanced surface requires less surface area than the unenhanced surface for the same amount of heat transfer. Consequently, a savings in the cost of material and labor is achieved by reducing the surface area required.

Enhanced surfaces have been classified by Yilmaz and Westwater [Ref. 1] into two groups: (1) Porous coatings, and (2) Integral machined surfaces. Several techniques utilized in the production of porous surfaces, as reported by Bergles and Chyu [Ref. 2] are: poor welding, sintering or brazing of particles, electrolytic deposition, flame spraying, bonding of particles by plating, galvanizing, or metallic coating of a foam substrate. One method utilized in the production of integral machined surfaces is described by Webb [Ref. 3] as follows:

> State-of-the art concepts employ cold metal working t form a high area density of reentrant nucleation site which are interconnected below the surface. Typicall these are reentrant grooves or tunnels, rather than discrete cavities.

Although the manner in which these two classes of surfaces enhance boiling heat transfer is not fully understood, useful information still can be found in the literature about their performance, and this is presented below.

The heat transfer mechanisms which have been postulated for boiling from porous coated surfaces have been generalized by Bergles and Chyu [Ref. 4] as follows:

> ...steady vapor formation in a porous matrix is considered to be primarily internal. There are preferential vapor escape channels, the liquid is supplied primarily through other channels surrounding the vapor channel. Evaporation occurs at the mouths of the liquid channels and on adjacent surfaces wetted by the liquid. A low ΔT is required for evaporation due to the large internal surface area. The vapor which is seen in the pool represents bubbling, as if air were blown into the pool through a perforated plate, rather than the conventional nucleate boiling cycle of nucleation, growth, and departure.

In the case of the machined integral surfaces, similar mechanisms may occur.

One particular integral machined surface which has received attention recently is the Gewa-T surface manufactured by Wieland-Werke, AG. During 1981, investigations of nucleate pool boiling from a Gewa-T surface were conducted by Yilmaz and Westwater [Ref. 5], Marto and Lepere [Ref. 6], and Stephan and Mitrovic [Ref. 7]. Yilmaz and Westwater compared the heat transfer performance of a Gewa-T surface to a plain copper tube in isopropyl alcohol. Their results show that at a heat flux of 40 kW/m^2, the heat transfer coefficient of the Gewa-T surface was 2.0 times that of the plain tube. Marto and Lepere compared the heat transfer performance of the Gewa-T surface to that of a plain copper tube in Freon-113 and FC-72. Their investigation spanned a heat flux range between 100 W/m^2 and 100 kW/m^2. Their investigation shows that for Freon-113 at low heat fluxes the Gewa-T surface improves the heat transfer coefficient over the plain surface by a factor of 2.5, and at high heat fluxes by a factor of 3. Marto and Lepere also determined that the degree of superheat required to activate nucleation on the Gewa-T surface is sensitive to initial surface treatment and fluid properties. Stephan and Mitrovic compared the heat transfer performance between a Gewa-T tube and a standard finned Gewa tube in R-11, R-12, R-22, and R-114. Their investigation covered a heat flux range between 5 W/m^2 and 10 kW/m^2. The results of their

investigation show the heat transfer coefficients of the Gewa-T surface are higher than those of a tube with straight fins of the same diameter and same fin side area. Recently, Stephan and Mitrovic [Ref. 8] have postulated that the increase in the heat transfer coefficient of the Gewa-T tube over the standard finned Gewa tube occurs in the following manner:

> A single vapor bubble, formed inside the T-shaped channel of the Gewa-T tube after break-off flows around the tube ... thus keeping contact with the tube along a path which is obviously longer than the contact length around the Gewa tube with plain fins.
>
> One can imagine therefore, that the bubbles when moving around the tube sweep off other forming bubbles still in growth. Thus the bubble frequency and also the heat transfer coefficients increase. For higher heat flux densities the large number of bubbles within the channel grow together forming a continuous vapor stream in the core, whereas a thin liquid film exists near the wall.
>
> The flow pattern around the tube seems to be of very weak influence and the heat transfer process is mainly governed by the bubble formation and the two phase flow inside the T-shaped channel. The top part of the fins, which were rolled to form the T, practically did not contribute to the heat transfer process, because even at maximum heat fluxes vapor bubbles were not produced there.

These investigations provide an indication of the nucleate boiling heat transfer performance of a Gewa-T surface, using several liquids and various experimental procedures. Due to the sensitivity to initial surface treatment and fluid properties exhibited by the Gewa-T surface, it is not possible at present to generalize the heat transfer mechanisms involved in nucleate pool boiling from a Gewa-T surface based on the

results of the investigations discussed. However, the postulate proposed by Stephan and Mitrovic is suited to experimental testing.

B. THESIS OBJECTIVES

The objectives of this thesis are therefore as follows:

1. Design and construct a test tube from a Gewa-T finned, solid, copper rod which will permit examination of nucleate pool boiling from a Gewa-T surface in Freon-113.

2. Gather experimental information to assist in understanding the physical mechanisms which give rise to increased heat transfer coefficients with this type of surface.

II. EXPERIMENTAL DESIGN

A. REQUIREMENTS GOVERNING DESIGN

The purpose of the experimental apparatus was to investigate nucleate pool boiling from a Gewa-T surface and attempt to ascertain the physical mechanisms which give rise to this phenomenon. Consequently, it was important to obtain reliable measurements of those parameters which may provide an indication of the nucleate boiling mechanism. These parameters established the minimum requirements governing the design of the apparatus. The parameters selected for measurement were as follows:

1. Ambient pressure
2. Surface heat flux
3. Test section wall temperature distribution
4. Vapor temperature
5. Fluid bulk temperature

B. TEST APPARATUS

The test apparatus and its major components are illustrated in Figure 1, and photographs of the apparatus are shown in Figures 2 and 3. The test liquid was chosen to be Freon-113.

1. Boiler

The boiler vessel was composed of a thick-walled pyrex glass container and a plexiglas cover fitted with a rubber

o-ring. The vessel had an outside diameter and a height of 305 mm, and these dimensions permitted variations in test section height or liquid level. The vessel was made of glass to provide an unobstructed view of the test section and fluid during the collection of data, and it was situated on top of an electric hot plate which served as the boiler heating element. The hot plate was utilized to pre-boil Freon-113 for degassing prior to the collection of data, and to maintain the fluid at saturation temperature during operation. Air and noncondensable gases produced from the degassing process were expelled to the atmosphere through a vent identified in Figure 1. The vent to the atmosphere permitted the boiler to achieve and maintain saturation conditions at ambient pressure, and consequently prevented pressurization of the boiler.

2. Condensers

The vapor produced from boiling was condensed with the use of a copper primary condenser and a glass secondary condenser. The condensers were water-cooled, and the condenser cooling water lines were connected in series. The condensed vapor was returned to the liquid bath through the action of gravity. Consequently, the recovery action of the condensers minimized the escape of Freon-113 to the atmosphere as a result of venting during boiling, and assisted in maintaining the conditions of saturation.

3. Test Section

Figure 4 illustrates a cutaway cross sectional view of the test section. The outside diameter of the test section was 21.2 mm and its total length was 114.1 mm. The Gewa-T surface length was 49.0 mm. A description of the manufacture, assembly, and calibration of the test section follows.

A spirally finned, solid, copper rod designated Gewa-T 13515.16, manufactured by Wieland-Werke AG, was utilized in this experiment. Figure 5 illustrates the fin profile of this surface. The characteristic T-shaped fins were formed by rolling a standard finned Gewa surface. The neighboring T-shaped fins of this surface form a series of tightly wound spiral channels.

a. Machining of Test Section

A radially-centered hole was drilled through the length of the solid copper rod to accommodate a cylindrical cartridge heater. Consequently, a tube with an inside diameter of 13.3 mm was manufactured from the solid rod. Next, eight longitudinal holes parallel to the tube axis were drilled in the tube wall up to the axis midpoint at a radius of 8.0 mm. All eight holes had a constant diameter of 1.6 mm. Seven of the eight holes were drilled at intervals of 30 degrees from each other such that they spanned an arc of 180 degrees. The eighth hole was centered at an interval of 90 degrees from either of the two nearest holes. Figure 6 illustrates the angular and radial position of the holes in

the tube wall. The Gewa-T surface was then machined off at each end of the tube, producing two unenhanced tube ends with an outside diameter of 19.0 mm, and a length of 31.9 mm. Next, the inside wall of the unenhanced ends was bored out such that the inside diameter of the ends was increased to 18.3 mm. Consequently, the wall thickness of the unenhanced ends was reduced to 0.35 mm, creating a thin-walled fin at each end. This action was taken to minimize longitudinal conduction losses from the test section.

b. Thermocouple Assembly

Eight copper-constantan thermocouples were manufactured from 0.1 mm diameter, teflon-insulated thermocouple wires. The average thermocouple bead diameter was 0.5 mm. These thermocouples were inserted into eight soft copper capillary tubes whose outside and inside diameters were 1.6 mm and 0.6 mm respectively, and whose outside surfaces were tinned with Eutectic Corporation 157 solder. The thermocouples were soldered to the capillary tube end through which they protruded such that the face of the tube end served as a base for attachment.

c. Soldering of Thermocouples and Cartridge Heater in Test Section

A cylindrical cartridge heater was radially and axially centered in the test section with an aluminum plug which had a machined cavity on its interior face to accept the heater. This assembly was fitted through an aluminum stand and placed on top of an electric hot plate which had

been heated for approximately 25 minutes. The hot plate was then further heated to a temperature of approximately 350 °C in order to bring the test section to the melting temperature of solder which was 218 °C. Next, a bead of melted solder was dropped into each of the eight holes bored into the tube wall. The tinned capillary tubes were then inserted into these eight holes and soldered into place. This procedure was immediately followed by soldering the cartridge heater into place using the same Eutectic Corporation 157 solder. Upon completion of the soldering process, the assembly was removed from the hot plate and quenched under flowing tap water.

d. Insulation of Test Section Ends

After the test section was cooled to ambient temperature and dried, the aluminum plug was removed and replaced with a teflon plug of the same dimensions. The end through which the heater and thermocouple wires protruded was insulated with poured epoxy resin. The thin-wall surface at the teflon plug end was scribed to indicate the angular position of the thermocouples.

4. Calibration of Thermocouples

Next, the 0.1 mm diameter copper-constantan thermocouple wires were welded to 0.3 mm diameter extension wires, and covered with heat shrinkable tubing. The thermocouple wires were wrapped to the heater wires with insulation tape. The test assembly was placed in a Rosemont distilled water constant temperature bath, and the thermocouples were connected

to a Newport digital pyrometer through a 16-pole thermocouple switch. Two separate copper-constantan thermocouples were also placed in the bath and connected to the same Newport pyrometer. The test section thermocouples, the two separate thermocouples, and the Newport digital pyrometer were then calibrated as a system against a platinum resistance thermometer at a given bath temperature. Each thermocouple temperature measurement was individually read with the use of the thermocouple switch mentioned above. The calibration temperature range was between 39.23 °C and 90.33 °C. The bath temperature was increased in increments of approximately 10 °C and then decreased in similar increments, except for an initial decrease of 6 °C.

The calibration of each thermocouple was performed by plotting the difference in temperature between the thermocouple and the platinum resistance thermometer as a function of thermocouple temperature. The curve which best fit this data was a straight line generated from a least squares fit.

Symbolically, the difference in temperature between each thermocouple and the platinum resistance thermometer is:

$$\Delta T = T_{TC} - T_P \quad (°C) \qquad (1)$$

where:

T_{TC} = thermocouple temperature (°C),

T_P = platinum resistance thermometer temperature (°C),

ΔT = difference in temperature between thermocouple and platinum resistance thermometer (°C).

A least squares fit applied to the data yields:

$$\Delta T = A\, T_{TC} + B \quad (°C) \tag{2}$$

where A and B are constant coefficients. Therefore, the calibrated thermocouple temperature is determined from:

$$T_{CAL} = T_{TC} - \Delta T \quad (°C) \tag{3}$$

where:

T_{CAL} = calibrated thermocouple temperature (°C).

The interval, or band, centered about each calibration curve within which 90% of the data were located determined the uncertainty in temperature measurement. The calibration curves yielded an uncertainty of ± 0.15 °C.

5. Installation of Test Section in Apparatus

At the completion of the calibration process, the test section was polished and cleaned by immersing it in a 10% solution of nitric acid in ethyl alcohol for five minutes. After properly drying the test section, the thermocouple and heater wires located at one end were inserted into a

copper tube fitted with a Swagelok fitting. The copper tube had a gently sloping elbow of 90 degrees and served as a support arm for the test section. The Swagelok fitting secured the test section to the support arm.

The support arm and the two calibrated thermocouples were secured to the plexiglas cover on the boiler vessel. One of the two thermocouples was immersed in the freon pool to monitor the liquid bulk temperature, and the other was placed above the boiling fluid to measure the vapor temperature.

6. Other Instrumentation

The test section cartridge heater voltage was measured with a digital voltmeter, accurate to 0.01 volts. The heater current was determined by measuring the voltage drop across a 2.031 ohm precision resistor which was connected in series with the cartridge heater.

. SHROUDS

Four aluminum shrouds were manufactured with an outside diameter of 22.2 mm and a wall thickness of 0.45 mm. Each shroud measured 51.4 mm in length and had two diametrically opposed windows of various aperture angles. The two windows on each shroud subtended arcs of the following combinations: 60 degrees and 60 degrees, 30 degrees and 30 degrees, 60 degrees and 30 degrees, 60 degrees and 8.5 degrees. The shrouds were slipped over the test section, providing a tight mechanical fit, and they were oriented with the larger aperture centered vertically at the top of the test section.

III. EXPERIMENTAL PROCEDURES

The work of Bergles and Chyu [Ref. 9] and Marto and Lepere [Ref. 6] show the dependence of boiling incipience on surface past history, or on surface treatment. Therefore, it was necessary to establish a procedure which could be easily and reliably repeated, and which would permit the comparison of data.

A. PROCEDURE A

Procedure A required the test section to be immersed in the liquid pool overnight. The liquid level was maintained at a height of 101.6 mm, and the height of the test section from the base of the glass vessel to the test section axis was 50.8 mm. At the start of the run, the hot plate voltage was adjusted to the maximum setting and was used to degas the fluid by vigorously boiling the pool for one hour. The plate voltage was then reduced to minimize the boiling intensity and maintain the pool at its saturation temperature. Power was then supplied to the test section heater by adjusting its voltage. The heater voltage was increased in increments between 2 and 30 volts, and then decreased in increments of approximately 10 volts. The system was allowed to stabilize for 5 minutes at each power setting and the following data were recorded: heater voltage, precision resistor voltage, vapor temperature, liquid pool temperature, and the eight test section wall temperatures.

B. PROCEDURE B

Procedure B did not require the test section to be immersed in the pool overnight. Instead, the test section was immersed in the pool and subjected to pre-boiling at 30 kW/m^2 for one hour using the cartridge heater while the hot plate voltage was adjusted to the maximum setting. Immediately after this one hour surface aging treatment, the power to the test section heater and the plate heater was secured, and both the test section and the fluid were allowed to cool for one-half hour. The plate heater voltage was then adjusted to the saturation temperature setting, and the cartridge heater voltage was adjusted in various increments as described under Procedure A. At each power setting, the same data as describe under Procedure A were recorded.

C. PROCEDURE EMPLOYMENT AND TYPES OF RUNS

Procedure A was employed only once. It was used to compare the data obtained in the current investigation to the data of Lepere [Ref. 10] and to observe any indication of the effect test section diameter may have on the heat transfer coefficient. In this investigation, the outside diameter of the test section was 21.2 mm, whereas the test section of Lepere had an outside diameter of 17.9 mm.

Procedure B was utilized in all the other data runs. Two data runs utilizing Procedure B were made to verify the reproducibility of the results obtained. For this reproducibility investigation, the test section height was 50.8 mm

from the base of the glass vessel to the test section axis, and the liquid level was maintained at a height of 101.6 mm. In two other reproducibility tests, the test section was lowered to a height of 38.1 mm in one data run, and raised to a height of 76.2 mm in the other. The data obtained from these two runs were compared to the data in which the test section height was 50.8 mm. A final reproducibility test was performed with the test section rotated 90 degrees, and at a height of 50.8 mm. The results obtained were compared against those data obtained at the same height but without the rotation. The effects on nucleate pool boiling due to the channels formed by neighboring T-shaped fins, and the fin geometry, were studied utilizing Procedure B.

The channel effect was investigated in four separate data runs by fitting a different shroud over the test section for each run. The fin effect was studied by progressively machining away the fin height in three consecutive data runs. In one data run the fin "T-caps" were removed; in another data run the fin height was reduced to 0.2 mm above the base surface; and in the remaining data run, the fins were completely removed, and the tube was mechanically polished with emery cloth and jeweler's rouge to a mirror finish.

D. TEMPERATURE CALCULATIONS

The saturation temperature was determined from the thermocouple which measured the vapor temperature. The surface temperature of the test cylinder wall was extrapolated from

the calibrated temperature measurements of the eight thermocouples imbedded in the tube wall.

The surface temperature was assumed to be the temperature at the base of the fins. The wall temperature was computed by taking the average of the eight calibrated wall thermocouple measurements, and then a correction was applied for the temperature drop across the tube wall due to conduction in the test cylinder. Therefore, the surface wall temperature is:

$$T_b = T_{AVG} - q\left(\frac{\ln \frac{r_2}{r_1}}{2\pi L k_c}\right) \quad (°C) \qquad (1)$$

where:

T_b = wall temperature at the base of the fins (°C),

T_{AVG} = average calibrated thermocouple temperature (°C),

$$T_{AVG} = \left(\sum_{n=1}^{8} T_n\right)/8.0 \ (°C) \qquad (2)$$

r_1 = radius of thermocouple position (m),

r_2 = radius of the test section to the base of the fins (m),

k_c = thermal conductivity or copper (W/m -°C),

L = length of the enhanced surface (m),

q = heat transfer rate (W).

The heat transfer rate was determined by computing the power to the test section heater in the following manner:

V = cartridge heater voltage (volts),

V_{RES} = precision resistor voltage drop (volts),

R = resistance of precision resistor (ohms),

$$I = V_{RES}/R \quad \text{(amps)} \tag{3}$$

$$q = V\,I \quad \text{(W)}. \tag{4}$$

E. HEAT FLUX CALCULATIONS

The surface heat flux was determined by subtracting the heat losses due to longitudinal heat conduction through each of the unenhanced thin-walled ends from the power supplied to the test cylinder heater, and then dividing the difference by the area of the test surface at the base of the fins. It was assumed that free convection from a horizontal cylinder was applicable to the unenhanced ends. The average heat transfer coefficient of the unenhanced ends was then determined from the appropriate Churchill and Chu correlation [Ref. 11] for the average Nusselt number:

$$Nu_{D_o} = \left\{ 0.60 + \frac{0.387\ Ra_{D_o}^{1/6}}{[1 + (0.559/Pr)^{9/16}]^{8/27}} \right\}^2 \tag{5}$$

$$10^{-5} < Ra_{D_o} < 10^{2}.$$

The average Nusselt number is:

$$Nu_{D_o} = \frac{\bar{h} D_o}{k} . \tag{6}$$

Therefore, the average heat transfer coefficient is:

$$\bar{h} = \frac{k}{D_o} \left\{ 0.60 + \frac{0.387 \, Ra_{D_o}^{1/6}}{[1 + (0.559/Pr)^{9/16}]^{8/27}} \right\}^2 \tag{7}$$

where:

k = thermal conductivity of Freon-113 (W/m - °C),

D_o = outside tube diameter at unenhanced ends (m),

ν = kinematic viscosity (m^2/s),

α = thermal diffusivity (m^2/s)

$$Pr = \frac{\nu}{\alpha} \tag{8}$$

$$Ra_{D_o} = \frac{g\beta(\overline{T_W - T_{SAT}}) D_o^3}{\nu^2} \tag{9}$$

T_W = unenhanced surface wall temperature (°C),

T_{SAT} = fluid saturation temperature (°C),

$\overline{T_W - T_{SAT}}$ = average difference between surface wall temperature and fluid saturation temperature (°C),

g = gravitational acceleration (m/s^2),

β = volumetric thermal expansion coefficient (1/°C)

$$= -\frac{1}{\rho} \frac{\Delta\rho}{\Delta T} \quad (1/°C) . \tag{10}$$

In equation (9), however, $(\overline{T_W - T_{SAT}})$ is not explicitly known.

The thin-walled ends were modeled as rectangular fins with insulated tips, in order to determine the heat loss q_ℓ from the ends. Therefore, the heat loss from a thin-walled fin with an insulated tip at each end of the test section is computed from the following equation found in Incropera and Dewitt [Ref. 12]:

$$q_\ell = [\bar{h} P k_c A]^{1/2} \theta_b \tanh mL_c \quad (W) \tag{11}$$

where:

P = tube outside wall perimeter (m),

$$P = \pi D_o \quad (m) \tag{12}$$

k_c = thermal conductivity of copper (W/m - °C),

A = tube cross-sectional area (m^2)

$$A = \frac{\pi}{4}(D_o^2 - D_i^2) \quad (m^2) \tag{13}$$

D_i = inside tube diameter at unenhanced ends (m),

t = fin thickness (m),

$$t = (D_o - D_i) \quad (m) \tag{14}$$

L_c = Harper-Brown length correction (m),

$$L_c = L_u + \frac{t}{2} \quad (m) \tag{15}$$

L_u = length of unenhanced surface (m),

$$m = \left(\frac{\bar{h}\,P}{k_c A}\right)^{1/2} \quad (1/m) \tag{16}$$

It was assumed that the temperature at the base of the thin-walled fin was equal to the temperature at the base of the Gewa-T fins. Therefore:

$$\theta = T_W - T_{SAT} \quad (°C) \tag{17}$$

$$\theta_b = \theta(0) = T_b - T_{SAT} \quad (°C) \tag{18}$$

and

$$\frac{\theta}{\theta_b} = \frac{\cosh m(L_c - x)}{\cosh mL_c} . \tag{19}$$

The average difference between the wall temperature and the saturation temperature may now be determined from the temperature distribution equation as follows:

$$\theta = \frac{\theta_b \cosh m(L_c - x)}{\cosh mL_c} \quad (°C) \tag{20}$$

$$\bar{\theta} = \frac{1}{L_c} \int_0^{L_c} \theta_b \frac{\cosh m(L_c - x)}{\cosh mL_c}\, dx \quad (°C) \tag{21}$$

$$\bar{\theta} = \frac{\theta_b}{mL_c} \tanh mL_c \quad (°C)$$

$$= \overline{T_W - T_{SAT}} \quad (°C) \tag{22}$$

However, m is a function of $\bar{h}$, and $\bar{h}$ is a function of $\bar{\theta}$. This yields a transcendental equation for $\bar{h}$:

$$\bar{h} = \frac{k}{D_o}\left\{0.60 + \frac{0.387\left(\frac{g\beta\bar{\theta}D_o^3}{\nu\alpha}\right)^{1/6}}{\left[1 + (0.559/Pr)^{9/16}\right]^{8/27}}\right\}^2 \quad (W/m^2 - °C) \qquad (23)$$

$$\bar{h} = \frac{k}{D_o}\left\{0.60+0.387\ \frac{\left(\frac{g\beta\theta_b\left[\tanh\left(\frac{\bar{h}P}{k_cA}\right)^{1/2}L_c\right]D_o^3}{\left(\frac{\bar{h}P}{k_cA}\right)^{1/2}L_c\,\nu\alpha}\right)^{1/6}}{\left[1 + (0.559/Pr)^{9/16}\right]^{8/27}}\right\}^2 \qquad (24)$$

$$(W/m^2 - °C)$$

The value of $\bar{h}$ is determined by an iterative technique. An initial guessed value for $\bar{h}$ is substituted into the right hand side of equation (24), and a new value $\bar{h}'$ is computed. The new value $\bar{h}'$ is now subtracted from the old value. If the difference is less than .001, then the value of $\bar{h}$ has been determined; otherwise, the new $\bar{h}'$ is substituted into the right hand side of the above equation and this process continues until the difference is less than .001.

Once $\bar{h}$ is computed, the heat loss may be determined by substituting the value of $\bar{h}$ into equation (11). After the heat loss is determined, the corrected heat transfer rate from the test section is computed as follows:

$$q_c = q - 2q_\ell \quad (W) \qquad (25)$$

Therefore, the corrected heat flux from the test surface is:

$$q'' = \frac{q_c}{2 \pi r_2 L} \quad (W/m^2) \tag{26}$$

IV. RESULTS AND DISCUSSIONS

Thirteen experimental runs were made. The data obtained are illustrated in the figures provided, and the figures are arranged in the order of the following discussion.

A. COMPARISON WITH DATA OF LEPERE [REF. 10]

Procedure A, as described in Chapter III, was performed in exactly the same manner as reported by Lepere. However, the test cylinder used in this investigation had eight thermocouples soldered to the tube wall as described in Chapter II, whereas the test cylinder used by Lepere had four equidistant thermocouples soldered to the surface of his cylindrical cartridge heater. In addition, the outside diameter of the Gewa-T surface utilized in this work was 21.2 mm, whereas the outside diameter of the Gewa-T tube used by Lepere was 17.9 mm. The surface geometry of the two test cylinders was identical in all other respects.

Figure 7 illustrates the data of Lepere plotted together with the data collected in this investigation. The new data conform closely to the Lepere data, and a hysteretic behavior is observed in both sets of data. At low heat fluxes, the agreement is excellent; as heat flux increases, however, the Lepere data exhibit a heat transfer coefficient which is as much as 1.4 times the heat transfer coefficient of the Gewa-T surface utilized in this investigation. The present data

indicate that the heat transfer coefficient levels off in the high heat flux region at a faster rate than do the Lepere data. While a quantitative explanation of this behavior is not provided, a qualitative assessment of the data plotted supports the work of Cornwell, Schüller, and Einarsson [Ref. 13], which examines the effect of tube diameter on the heat transfer coefficient. They showed that increasing the outside tube diameter produces a decrease in the heat transfer coefficient.

B. REPRODUCIBILITY TESTS

The data obtained from the reproducibility tests described in Chapter III are illustrated in Figures 8, 9, 10, 11, and 12. Figure 8 is selected as the standard plot of the data collected utilizing procedure B; these data are plotted as a solid curve in all subsequent figures for the purpose of comparison. Figure 9 compares the reproducibility of two sets of data obtained utilizing Procedure B under identical conditions. The agreement is excellent. Figures 10 and 11 compare the data obtained from lowering the test section height and raising the test section height respectively, against the standard data depicted by a solid curve. Once again, the agreement is excellent, indicating that liquid level in the pool is not an important variable.

The final test of reproducibility is plotted in Figure 12. In this case, the test cylinder was rotated 90 degrees for the purpose of comparing any non-uniformities in the

peripheral wall temperature distribution. However, it was determined that the uncertainty in temperature measurement, which was ± 0.15 °C, did not permit a good comparison since the peripheral temperature variation was only approximately ± 0.30 °C. Therefore, the temperature data reveal the necessity of utilizing a more precise temperature measuring instrument in order to make a comparison possible. Figure 12, however, shows that the data obtained from rotating the test cylinder 90 degrees are in excellent agreement with the standard data.

It is apparent, therefore, that data may be reproduced utilizing Procedure B with excellent agreement to the standard data. There is no recognizable influence due to the height of the test section in the liquid, nor is there any apparent influence due to rotation of the test cylinder. The figures cited support the confidence placed in the data obtained.

C. CHANNEL EFFECT

The initial study of the channel effect on nucleate pool boiling was made by direct physical observation of the Gewa-T surface during operation. At low heat fluxes, bubbles were observed to flow out from between the channels located at the top of the tube. The direction of the bubble flow was up, toward the surface of the liquid. As the heat flux was increased, the bubble frequency was observed to increase, and bubbles of about 1.5 times the diameter of those leaving from

the top of the tube were observed flowing out from channels on the lower half of the Gewa-T surface. In addition, bubbles of nearly 3 times the size of those at the top were observed forming between the fin tips along the bottom of the tube. These large bubbles originated from smaller bubbles which were pushed out through the gap between the T-shaped fins. The bubbles remained situated between the fins and continued to grow at this location until they were eventually separated from the surface by the action of local convection currents. At high heat fluxes, the frequency of large bubble formation and the bubble efflux from channels along the bottom of the tube were so great that these bubbles essentially formed a vapor blanket on the bottom of the tube. Similarly, the frequency of formation and efflux of bubbles from the remaining channels on the lower half of the Gewa-T tube, and from the top of the Gewa-T tube also increased. This observation has not been reported in the literature to the best of the author's knowledge.

The observation made on bubble formation, growth, and efflux from the channels does not agree with the description provided by Stephan and Mitrovic. They explain that bubble formation and growth take place entirely within the channels, and bubbles only flow out from channel openings located toward the top of the Gewa-T surface. It was observed, however, that not all bubbles flow around and within the tube channels. Bubbles with a diameter less than that of the gap between the

fins flow through the gap and out into the liquid pool. In addition, at high heat fluxes, bubble nucleation was observed to occur at the outer surface of the fins, whereas Stephan and Mitrovic reported that they did not observe this condition during their investigation. This was most probably because their heat fluxes were substantially less than those used during the current investigation.

As heat flux is increased, bubble generation increases and more bubbles exit from between the channels. The bubbles exiting from between the channels at the bottom of the tube disrupt the liquid flow upward into the channels and eventually blanket the tube surface at the highest heat flux. Consequently, the heat transfer coefficient levels off. Therefore, if the bubbles can be constrained to flow only within the channels, an increase in the heat transfer coefficient is expected. The shrouds described in Chapter III were utilized to examine this effect.

The aluminum body of the shrouds closed the channel openings created by the fin gaps, and produced channels which constrained the bubbles and liquid to flow within the closed channels. The shroud windows permitted liquid to flow into the channels located at the bottom of the tube, and a two-phase mixture of liquid and vapor to flow out of the channels located at the top of the tube. The range of window aperture combinations manufactured was the result of pursuing a combination which would maximize the heat transfer coefficient.

Figures 13, 14, 15, and 16 illustrate the data obtained utilizing the shrouds. All of the window combinations increased the heat transfer coefficient at low heat fluxes. When the shrouds were fitted over the Gewa-T surface, it was observed that bubbles which form and grow between the fin tips at the bottom of the tube are pushed back through the channel openings created by the gap between the fins, and are circulated within the closed channels. Consequently, more bubbles are now available to remove other bubbles in the process of growth and formation as these bubbles circulate in the channel, giving rise to an improvement in the heat transfer coefficient when compared to an unshrouded surface. However, at high heat fluxes, the heat transfer coefficient decreased. This decrease may be explained by the high frequency of bubbles exiting from the channel openings at the bottom of the tube. These bubbles disrupt the flow of liquid into the channels, and the channel surfaces become liquid starved. Consequently, the thin liquid film which exists at high heat fluxes, as described by Stephan and Mitrovic [Ref. 7] is evaporated and the heat transfer coefficient is observed to decrease. A comparison of the improvement in the heat transfer coefficient between the unshrouded and the shrouded Gewa-T tube follows.

At a heat flux of 10 kW/m^2 the heat transfer coefficient was increased by 90 percent with the 60°-60° shroud, and by 111 percent with the 30°-30° shroud when compared to the tube without the shroud, as illustrated in Figures 13, and 14,

respectively. At the same heat flux, the heat transfer coefficient was increased by 123 percent with the 60°-30° shroud, and by 153 percent with the 60°-8.5° shroud when compared to the unshrouded tube, as illustrated in Figures 15, and 16, respectively.

At a heat flux of 100 kW/m^2, the heat transfer coefficient was observed to show no change with the 60°-60° shroud, but it decreased by 33 percent with the 30°-30° shroud when compared to the unshrouded tube, as illustrated in Figures 13, and 14, respectively. At the same heat flux, the heat transfer coefficient decreased by 20 percent with the 60°-30° shroud, and by 36 percent with the 60°-8.5° shroud when compared to the unshrouded tube as illustrated in Figures 15, and 16, respectively. Therefore, at low heat fluxes the bubble circulation in the channels is enhanced by the application of the shrouds which in turn enhances heat transfer. The improved circulation is due to the buoyant forces which propel the less dense vapor bubbles to the liquid surface at the channel opening. However, at high heat fluxes, the window apertures at the top of the tube were not sufficient to permit adequate flow of vapor-liquid out of the channels. Similarly, the bubbles exiting from the channel openings at the bottom windows, disrupted the liquid flow into the channels. In addition, the shroud body itself prevented liquid from flowing into those channels covered by the shroud. Consequently, the heat transfer coefficient was observed to decrease in the high heat flux region.

D. FIN EFFECT

The fin effect was investigated by progressively machining away the fin height. Figures 17, 18, and 19 illustrate the data obtained after removing the fin "T-caps," the fins, and polishing the unfinned tube to a mirror finish, respectively. A comparison of the heat transfer coefficients obtained with the machined geometries was made at a low heat flux of 10 kW/m^2 and at a high heat flux of 100 kW/m^2. The effect of surface roughness was examined by comparing the heat transfer performance between a mirror polished smooth surface with that of an unpolished smooth surface. Surface roughness produced an increase in the heat transfer coefficient of 90 percent at the low heat flux and an increase of 58 percent at the high heat flux. The addition of the fins to a smooth tube increased the heat transfer coefficient by only 5 percent at the low heat flux, and by 38 percent at the high heat flux. This implies that the addition of fins did not greatly enhance the heat transfer. The addition of the "T-caps" to the straight fins increased the heat transfer coefficient by 58 percent at the low heat flux, and by 50 percent at the high heat flux. Therefore, the heat transfer performance of the Gewa-T surface is predominantly influenced by the effect of the channels created by neighboring T-shaped fins.

V. CONCLUSIONS

(1) Bubbles were observed to burst out from between the fins on the lower half of the tube, and nucleation was observed to occur on the outer surface of the fins. Therefore, the vapor-liquid flow path is not confined entirely within the channels formed by the T-shaped fins as postulated by Stephan and Mitrovic.

(2) The effect of surface roughness was examined by comparing the data of the mirror polished smooth tube to that of the unpolished smooth tube. Surface roughness increases the heat transfer coefficient by 90 percent at low heat fluxes and by 58 percent at high heat fluxes.

(3) The addition of fins to the unpolished smooth tube increases the heat transfer coefficient by only 5 percent at low heat fluxes and by 38 percent at high heat fluxes.

(4) The addition of the "T-caps" to the straight fins increases the heat transfer coefficient by 58 percent at low heat fluxes and by 50 percent at high heat fluxes.

(5) The heat transfer coefficient of the Gewa-T surface may be increased by as much as 153 percent by using shrouds.

(6) An uncertainty in temperature measure of ± 0.15 °C did not permit comparison of the tube wall temperature profile. A temperature measuring instrument with a precision of at least 0.01 °C is required in order to compare wall temperature profiles.

VI. RECOMMENDATIONS

The following recommendations are made for further study of the nucleate pool boiling mechanism:

(1) A similar experimental study should be made with water as the boiling fluid. A comparison can then be made on the effect of bubble diameter between fluids with different surface tensions.

(2) A study should be made on the influence of the gap width on the heat transfer coefficient of a Gewa-T tube.

(3) A study should be made on the effect of surface irregularities (e.g., indentations along the fin surface) on external nucleation and on the heat transfer coefficient.

(4) Testing with shrouds should be continued to determine the optimum shroud which maximizes the heat transfer coefficient.

(5) A study should be made to compare the heat transfer performance between a standard-finned Gewa tube and a Gewa-T tube in order to examine the effect of fin geometry on tubes of equal surface area, and identical dimensions in all other respects.

APPENDIX A

PROPERTIES OF FREON-113 [REF. 14]

Boiling Point (14.7 psia)	117.63 (°F), 47.57 (°C)
Density, 116 (°F)	94.43 (lbm/ft^3)
Density, 118 (°F)	94.26 (lbm/ft^3)
Thermal Conductivity (100 °F)	0.0419 (BTU/hr-ft-°F)
Thermal Conductivity (120 °F)	0.0406 (BTU/hr-ft-°F)
Specific Heat (100 °F)	0.232 (BTU/lbm-°F)
Specific Heat (120 °F)	0.235 (BTU/lbm-°F)
Viscosity, 100 °F	1.379 (lbm/ft-hr)
Viscosity, 120 °F	1.229 (lbm/ft-hr)

APPENDIX B

SAMPLE CALCULATIONS

A. WALL TEMPERATURE AT THE BASE OF THE FINS

The surface wall temperature at the base of the fins is computed as follows:

$$T_b = T_{AVG} - q\left(\frac{\ln \frac{r_2}{r_1}}{2\pi L k_c}\right) \quad (°C)$$

where the measured parameters are:

$V = 20.74$ (volts)

$V_{RES} = 1.36$ (volts)

$R = 2.031$ (ohms)

$T_1 = 53.4$ (°C)

$T_2 = 53.4$ (°C)

$T_3 = 53.3$ (°C)

$T_4 = 53.4$ (°C)

$T_5 = 53.3$ (°C)

$T_6 = 53.3$ (°C)

$T_7 = 53.3$ (°C)

$T_8 = 53.4$ (°C)

$T_{SAT} = 47.6$ (°C)

$D_1 = 15.9$ (mm)

$D_2 = 19.3$ (mm)

$L = 49.0$ (mm)

$k_c = 383$ (W/m-°C)

Therefore,

$$I = V_{RES}/R = (1.36/2.031) = 0.67 \text{ (amps)}$$

$$q = V\,I = (20.74)(0.67) = 13.89 \text{ (W)}$$

$$T_{AVG} = \left(\sum_{n=1}^{8} T_n/8.0\right) = 53.4 \text{ (°C)}$$

$$T_b = T_{AVG} - q\left(\frac{\ln \frac{r_2}{r_1}}{2\pi L k_c}\right)$$

$$= 53.4 - 13.89\left(\frac{\ln \frac{19.3}{15.9}}{2\pi(0.049)(383)}\right) \text{ (°C)}$$

$T_b = 53.4$ (°C) (NOTE: In this example, the temperature drop is negligible.)

B. HEAT FLUX

The heat flux is now determined at the given heater voltage setting as given by:

$$q'' = \frac{q_c}{2\pi r_2 L} \quad (W/m^2)$$

where the parameters required are obtained as follows:

$$k(100\ °F) = 0.0419\ (BTU/hr\text{-}ft\text{-}°F)$$

$$k(120\ °F) = 0.0406\ (BTU/hr\text{-}ft\text{-}°F)$$

Linear interpolation at saturation temperature yields:

$$k(117.6\ °F) = 0.0419 + \left(\frac{117.6 - 100}{120 - 100}\right)(0.0406 - 0.0419)$$

$$(BTU/hr\text{-}ft\text{-}°F)$$

$$k(117.6\ °F) = 0.0408\ (BTU/hr\text{-}ft\text{-}°F), \text{ and}$$

converting k to SI units yields:

$$k(47.6\ °C) = (0.0408)(1.7296) = 0.0706\ (W/m\text{-}°C).$$

Similarly:

$$C_p(100\ °F) = 0.232\ (BTU/lbm\text{-}°F)$$

$$C_p(120\ °F) = 0.235\ (BTU/lbm\text{-}°F)$$

$$C_p(117.6\ °F) = 0.232 + \left(\frac{117.6 - 100}{120 - 100}\right)(0.235 - 0.232)\ (BTU/lbm\text{-}°F)$$

$$C_p(117.6\ °F) = 0.235\ (BTU/lbm-°F),$$

and converting C_p to SI units yields:

$$C_p(47.6\ °C) = (0.235)(4184) = 983.2\ (joule/kg-°C).$$

Similarly:

$$\mu(100\ °F) = 1.379\ (lbm/ft-hr)$$

$$\mu(120\ °F) = 1.209\ (lbm/ft-hr)$$

$$\mu(117.6\ °F) = 1.379 + \left(\frac{117.6 - 100}{120 - 100}\right)(1.209 - 1.379)\ (lbm/ft-hr)$$

$$\mu(117.6\ °F) = 1.229\ \ lbm-ft-hr,$$

and converting μ to SI units:

$$\mu(47.6\ °C) = (1.229)(0.00041338)\ \ (N-s/m^2)$$

$$\mu(47.6\ °C) = 5.080 \times 10^{-4}\ \ (N-s/m^2).$$

Similarly, for ρ:

$$\rho(116\ °F) = 94.43\ (lbm/ft^3)$$

$$\rho(118\ °F) = 94.26\ (lbm/ft^3)$$

$$\rho(117.6\ ^\circ F) = 94.43 + \left(\frac{117.6 - 116}{118 - 116}\right)(94.26 - 94.43) \quad lbm/ft^3$$

$$\rho(117.6\ ^\circ F) = 94.29\ (lbm/ft^3),$$

and converting ρ to SI units yields:

$$\rho(47.6\ ^\circ C) = (94.29)\left(\frac{0.4536}{(0.3048)^3}\right) \quad kg/m^3$$

$$\rho(47.6\ ^\circ C) = 1510.41\ (kg/m^3).$$

The kinematic viscosity is computed as follows:

$$\nu = \frac{\mu}{\rho} = \frac{5.080\ (10^{-9})}{1510.41} = 3.363\ (10^{-7})\ (m^2/s).$$

The thermal diffusivity is computed as follows:

$$\alpha = \frac{k}{\rho C_p} = \frac{0.0706}{(1510.41)(9.817)(10^2)} = 4.754\ (10^{-8})\ (m^2/s)$$

The volumetric thermal expansion coefficient is computed as follows:

$$\beta = -\frac{1}{\rho}\frac{\Delta\rho}{\Delta T} = \left(-\frac{1}{94.29}\right)\left(\frac{94.29 - 94.43}{117.6 - 116}\right)$$

$$\beta = 0.00093\ \left(\frac{1}{^\circ F}\right)$$

converting β to SI units yields:

$$\beta = (0.00093)(9/5) = 0.0017 \quad (\tfrac{1}{°C}).$$

The Prandtl number is computed as follows:

$$Pr = \frac{\nu}{\alpha} = \frac{3.363\ (10^{-7})}{4.754\ (10^{-8})}$$

$$Pr = 7.07.$$

The remaining parameters are:

$$g = 9.8 \quad (m/s^2)$$

$$D_o = (.749)(25.4) = 19.0 \quad (mm)$$

$$P = \pi D_o = 59.8 \quad (mm)$$

$$D_i = (0.720)(25.4) = 18.3 \quad (mm)$$

$$A = \pi(D_o^2 - D_i^2) = 8.202 \times 10^{-5} \quad (m^2)$$

$$t = (D_o - D_i) = 7.0 \times 10^{-1} \quad mm$$

$$L_u = (1.255)(25.4) = 31.9 \quad (mm)$$

$$L_C = L_u + \frac{t}{2} = 31.9 + \frac{0.7}{2} = 32.3 \quad (mm)$$

$$\vartheta_b = T_b - T_{SAT}\ (°C) = 53.4 - 47.6 \quad (°C)$$

$$\theta_b = 5.8 \quad (°C)$$

The average heat transfer coefficient is determined from:

$$\bar{h} = \frac{k}{D_o}\left\{0.60 + 0.387\frac{\left(\frac{g\beta\theta_b[\tanh(\frac{\bar{h}P}{k_cA})^{1/2}L_c]D_o^3}{(\frac{\bar{h}P}{k_cA})^{1/2}L_c\,\nu\,\alpha}\right)^{1/6}}{[1 + (0.559/Pr)^{9/16}]^{8/27}}\right\}^2$$

$$h = 190.746 \quad (W/m^2\text{-}°C)$$

The heat loss may now be computed from

$$q_\ell = [\bar{h}\,P\,k_cA]^{1/2}\,\theta_b \tanh mL_c$$

where:

$$mL_c = (\frac{\bar{h}P}{k_cA})^{1/2} = 0.60004$$

$$(\bar{h}\,P\,k\,A)^{1/2} = 0.61402$$

Therefore, the heat loss from each unenhanced end is:

$$q_\ell = 2.137 \quad (W)$$

The corrected heat transfer rate from the Gewa-T surface is:

$$q_c = q - 2q_\ell = 13.89 - 2(2.137) = 9.62 \text{ W}$$

The heat flux from the Gewa-T surface is:

$$q'' = \frac{9.62}{2.971\ (10^{-3})} = 3238 \quad (W/m^2)$$

APPENDIX C

UNCERTAINTY ANALYSIS

A. UNCERTAINTY IN SURFACE AREA

In order to determine the uncertainty in the surface area, it is necessary to first determine the uncertainty in the diameter at the base of the fins, and the uncertainty in the Gewa-T surface length.

$$\omega_{\ell} = \omega_{D_2} = 0.1 \quad (mm)$$

$$A = \pi D_2 L \quad (m^2)$$

where:

D_2 = diameter at the base of the fins (mm)

L = length of the Gewa-T surface

$$\frac{\partial A}{\partial D_2} = \pi L$$

$$\frac{\partial A}{\partial L} = \pi D_2$$

Consequently, the uncertainty in the surface area is:

$$\omega_A = [(\pi L \omega_{D_2})^2 + (\pi D_2 \omega_L)^2]^{1/2} \quad (m^2)$$

$$\omega_A = [(\pi(49.0)(0.1))^2 + (\pi(19.3)(0.1))^2]^{1/2}$$

$$\omega_A = [273.732]^{1/2} \quad mm^2$$

$$\omega_A = 16.5 \quad mm^2$$

The uncertainty in the surface area may be described in terms of a percentage of the surface area, as given below:

$$\frac{\omega_A}{A} = \frac{\omega_A}{\pi D_2 L}$$

$$\frac{\omega_A}{A} = \frac{16.5}{\pi(19.3)(49.0)}$$

$$\frac{\omega_A}{A} = 0.0056, \text{ or } 0.56 \text{ percent.}$$

B. UNCERTAINTY IN POWER

The uncertainty in power is determined from the uncertainties in the test section cartridge heater voltage and current. The measured uncertainties are as follows:

$$\omega_I = 0.01 \quad \text{(amps)}$$

$$\omega_V = 0.05 \quad \text{(volts)}$$

The uncertainty in power is computed as follows:

$$q = V\,I \quad (W)$$

$$\frac{\partial q}{\partial V} = I \quad (amps)$$

$$\frac{\partial q}{\partial I} = V \quad (volts)$$

$$\omega_q = [(I\omega_V)^2 + (V\omega_I)^2]^{1/2}$$

$$\omega_q = [((0.67)(0.05))^2 + ((20.74)(0.01))^2]^{1/2}$$

$$\omega_q = 0.21$$

The uncertainty in power may be expressed as a percentage of the power as given below:

$$\frac{\omega_q}{q} = \frac{\omega_q}{13.89} = 0.015, \text{ or } 1.5 \text{ percent}$$

C. UNCERTAINTY IN ΔT

The uncertainty in ΔT is determined from the uncertainty in temperature measurement. The uncertainty in temperature measurement is:

$$\omega_{T_W} = \omega_{T_{SAT}} = 0.15 \quad (°C)$$

$$\Delta T = T_W - T_{SAT}$$

$$\frac{\partial \Delta T}{\partial T_W} = 1.0$$

$$\frac{\partial \Delta T}{\partial T_{SAT}} = -1.0$$

Therefore, the uncertainty in ΔT is:

$$\omega_{\Delta T} = [(\omega_{T_W})^2 + (\omega_{T_{SAT}})^2]^{1/2}$$

$$\omega_{\Delta T} = [(0.15)^2 + (0.15)^2]^{1/2}$$

$$\omega_{\Delta T} = 0.2 \ ^\circ C$$

Expressed as a percentage of the temperature difference, the uncertainty in ΔT is:

$$\frac{\omega_{\Delta T}}{\Delta T} = \frac{0.2}{5.8} = 0.04, \text{ or } 4 \text{ percent.}$$

D. UNCERTAINTY IN HEAT FLUX

$$q'' = \frac{q - 2q_\ell}{A}$$

$$\frac{\partial q''}{\partial A} = -\frac{(q - 2q_\ell)}{A^2}$$

$$\frac{\partial q''}{\partial q} = \frac{1}{A}$$

$$\frac{\partial q''}{\partial q_\ell} = -\frac{2}{A}$$

$$\omega_{q''} = \left[\left(\left(\frac{-q+2q_\ell}{A^2}\right)(\omega_A)\right)^2 + \left(\left(\frac{1}{A}\right)(\omega_q)\right)^2 + \left(\left(-\frac{2}{A}\right)(\omega_{q_\ell})\right)^2\right]^{1/2}$$

As determined earlier, $\omega_A = 16.5$ and $\omega_q = 0.21$. In addition, it was assumed that $\omega_q \simeq 0.3q_\ell = 0.64$. Therefore, the uncertainty in heat flux is:

$$\omega_{q''} = \left[\left(\left(\frac{-9.62}{8.827(10^{-6})}\right)(16.5)\right)^2 + \left(\frac{0.021}{2.971(10^{-3})}\right)^2 + \left(\frac{2(0.64)}{2.971(10^{-3})}\right)^2\right]^{1/2}$$

$$\omega_{q''} = 437$$

The uncertainty in heat flux as a percentage of the total heat flux is:

$$\frac{\omega_{q''}}{q''} = \frac{437}{3238} = 0.135 \text{ or } 13.5 \text{ percent}$$

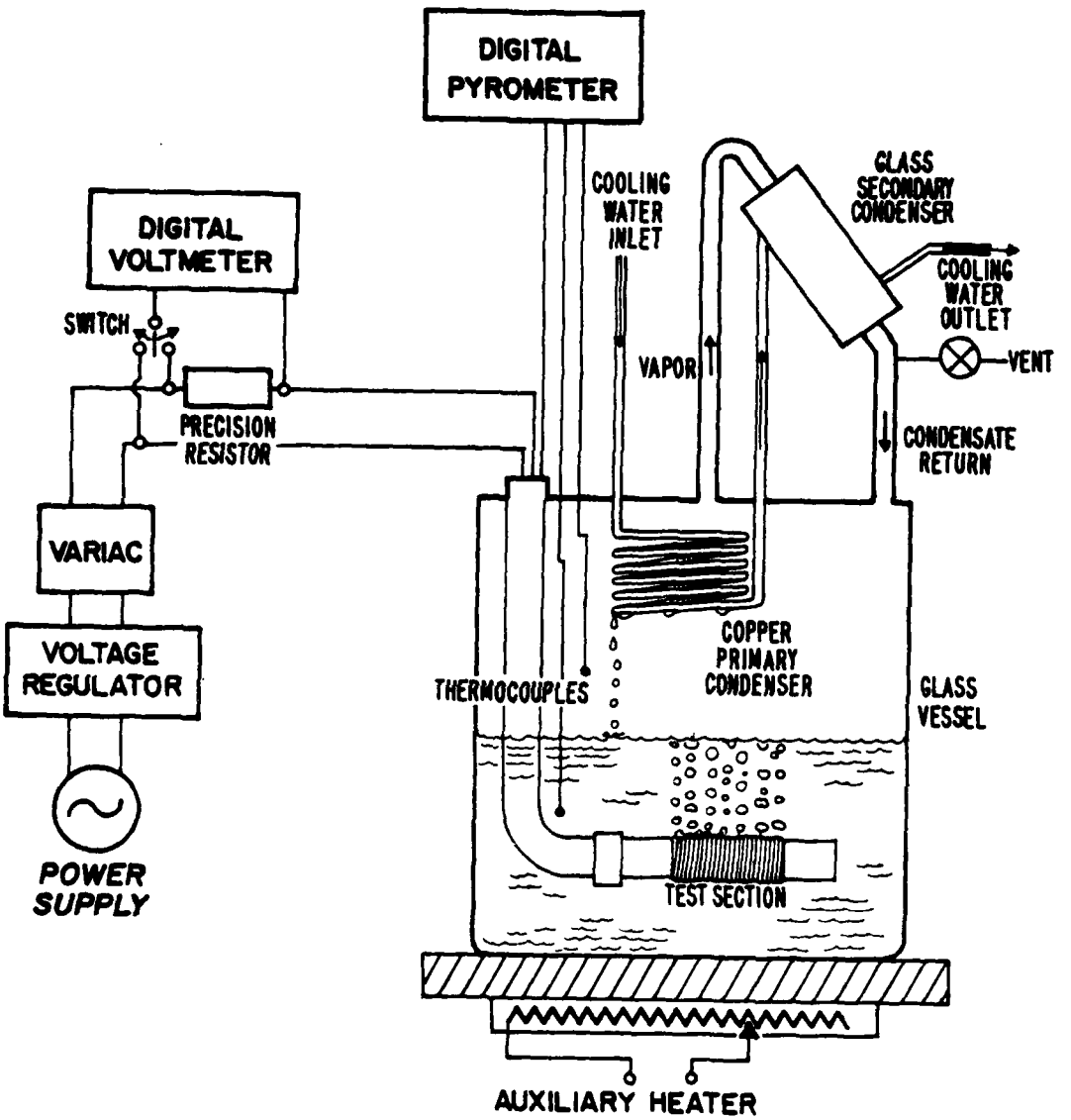

Figure 1. Schematic of Test Apparatus

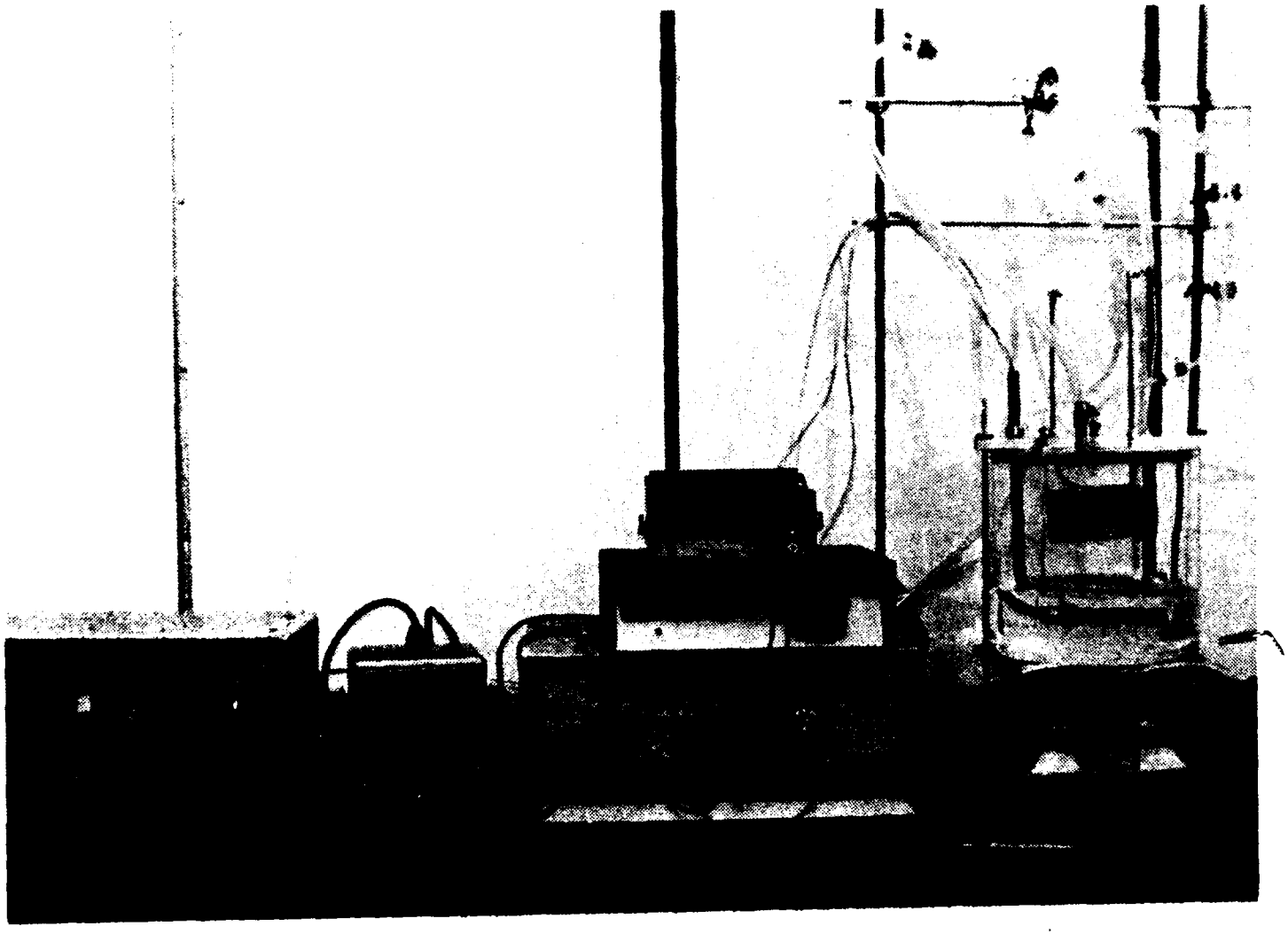

Figure 2. Photograph of Experimental Apparatus

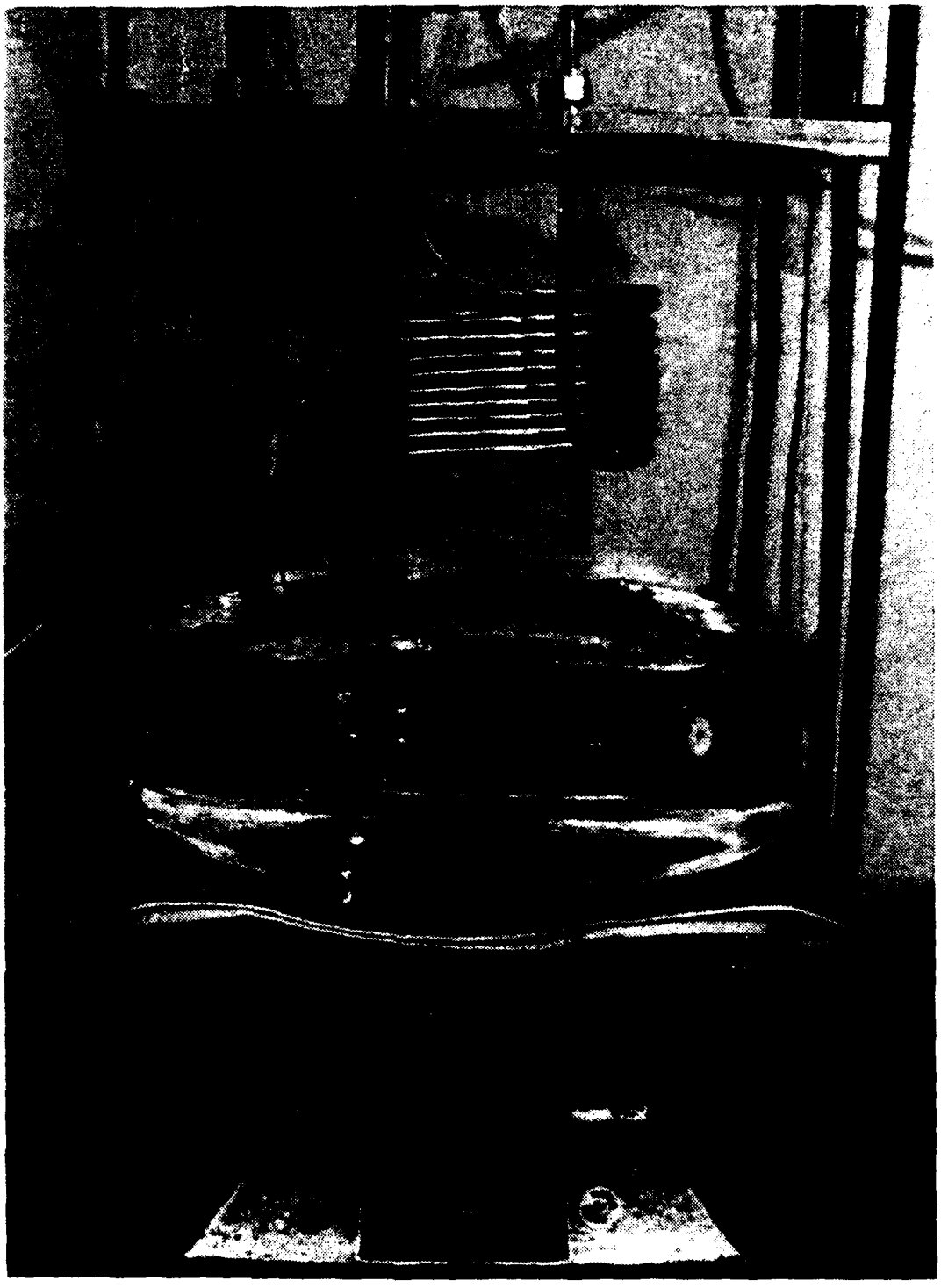

Figure 3. Photograph of Test Section in Boiler

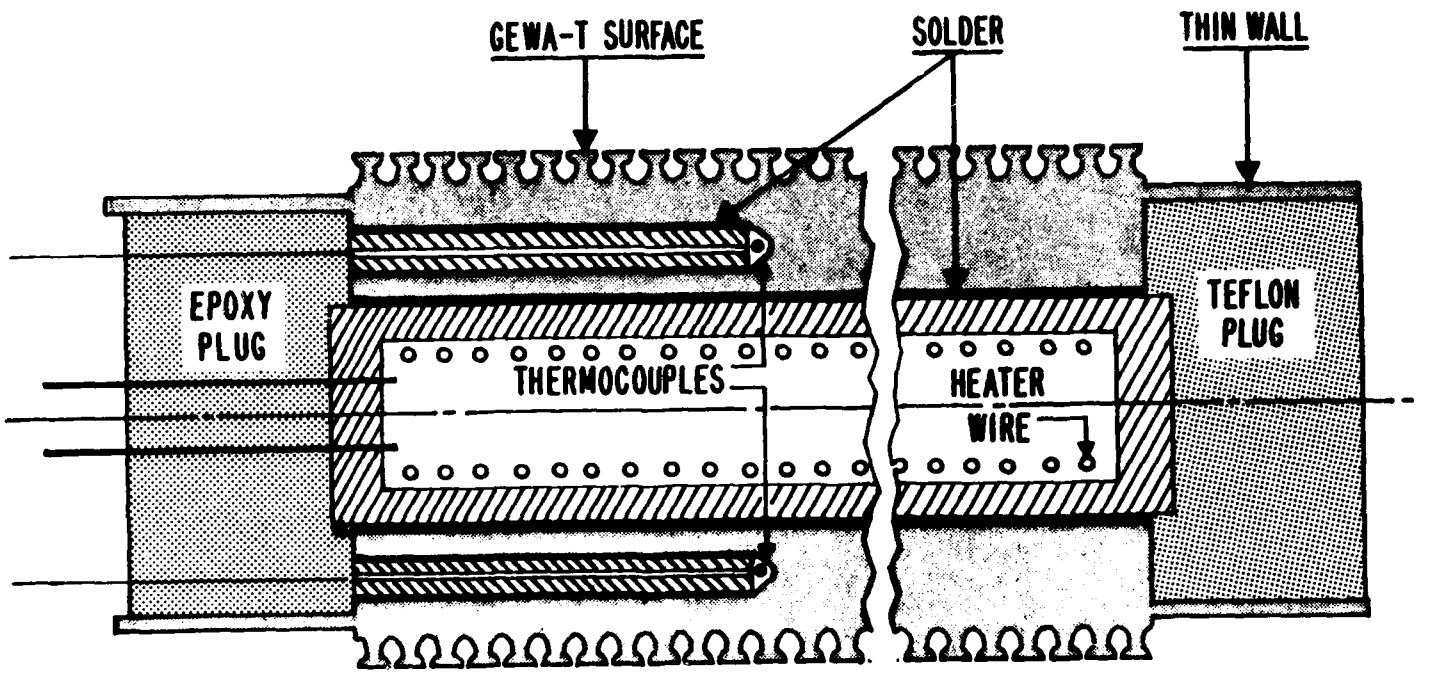

Figure 4. Cutaway Cross Sectional Representation of Test Section

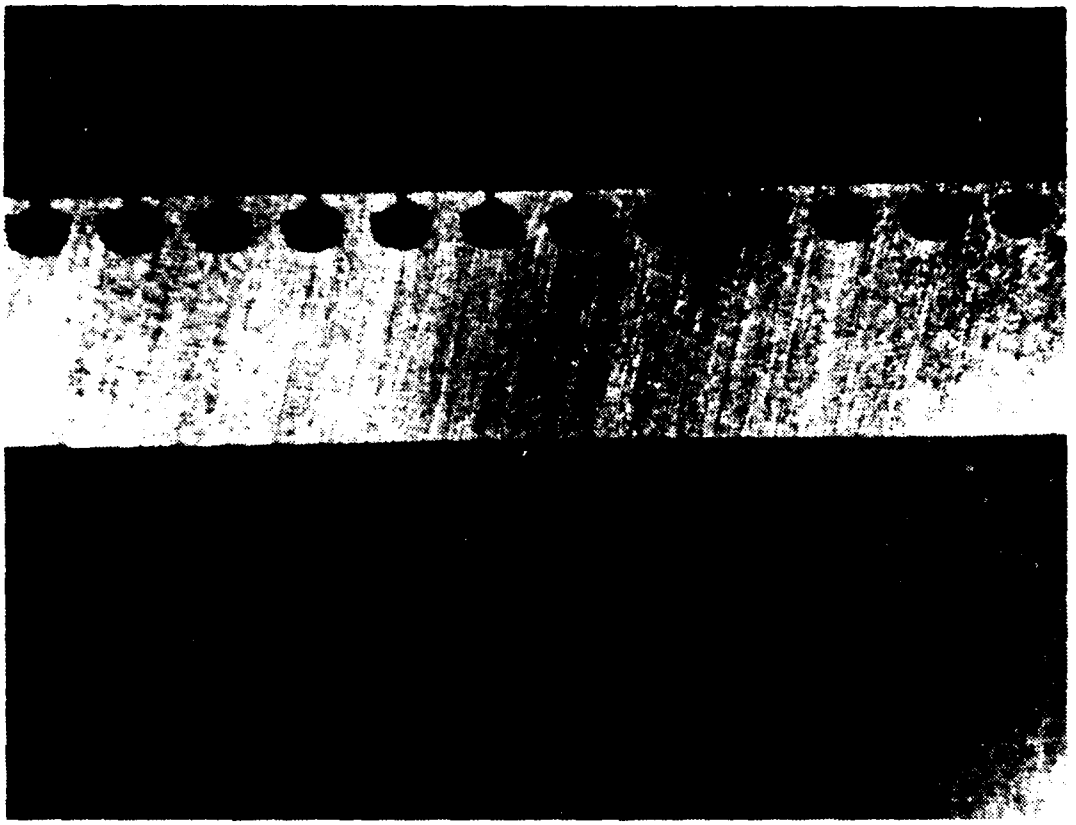

Figure 5. Optical Micrograph of Gewa-T Fin Profile, 7X

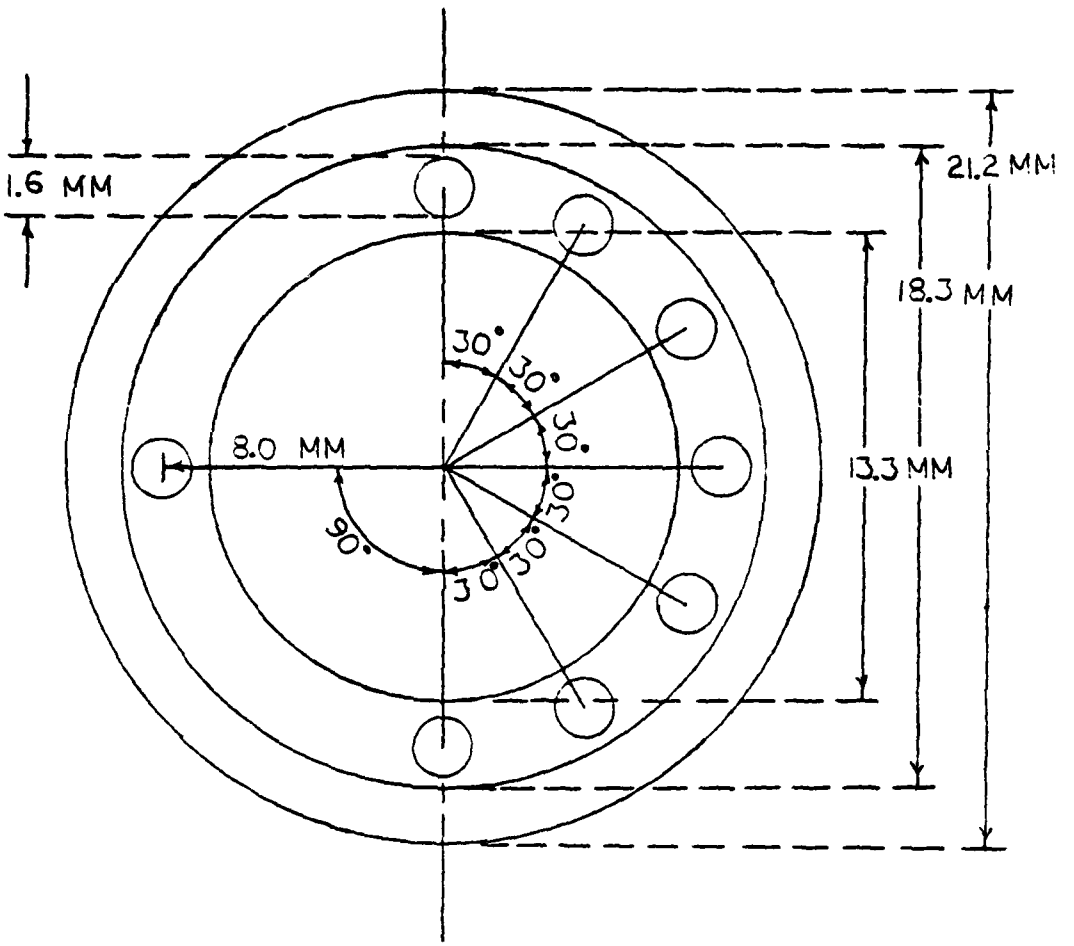

Figure 6. Thermocouple Radial and Angular Positions

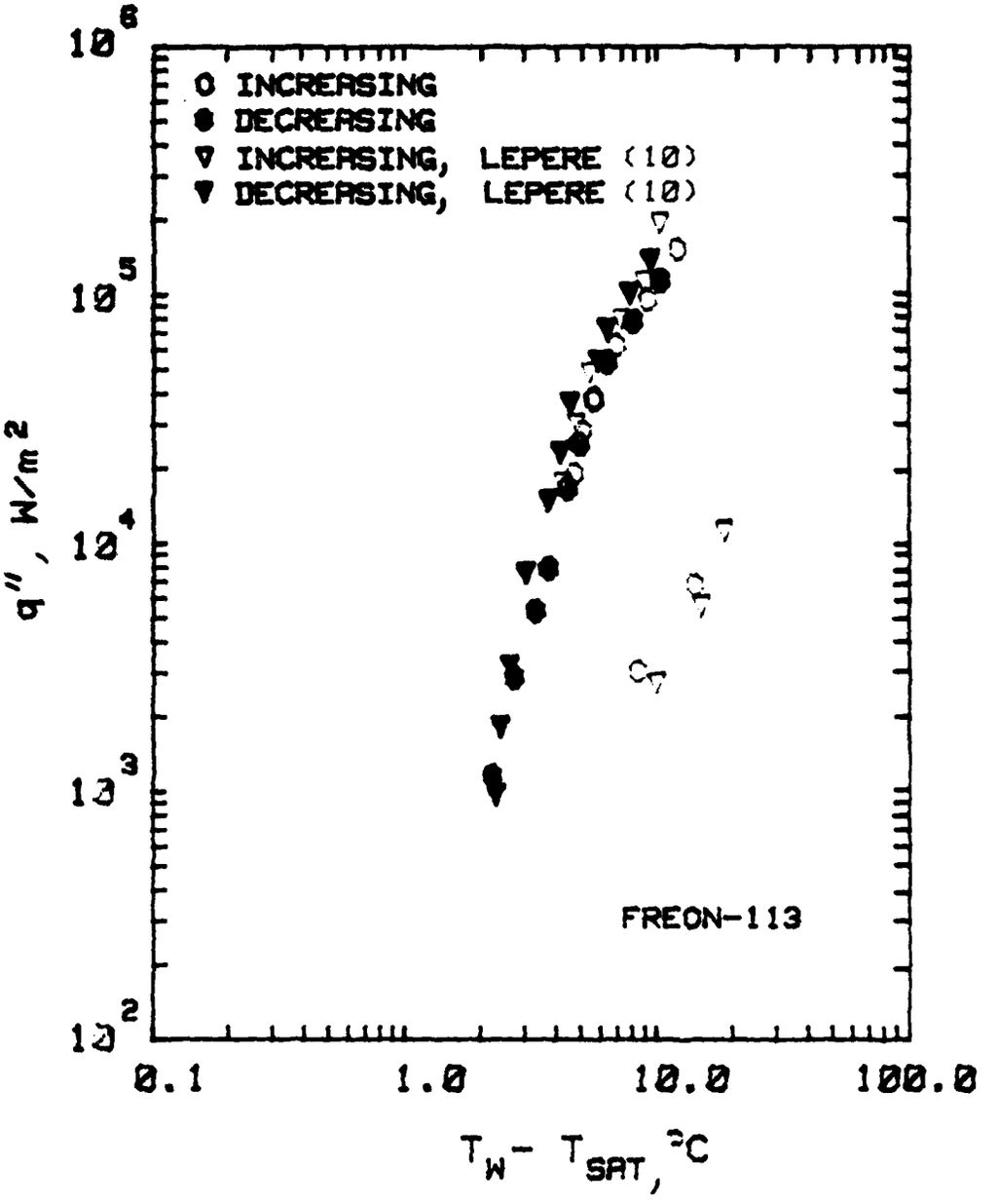

Figure 7. Procedure A: A Comparison of Present Data with that of Lepere [10]

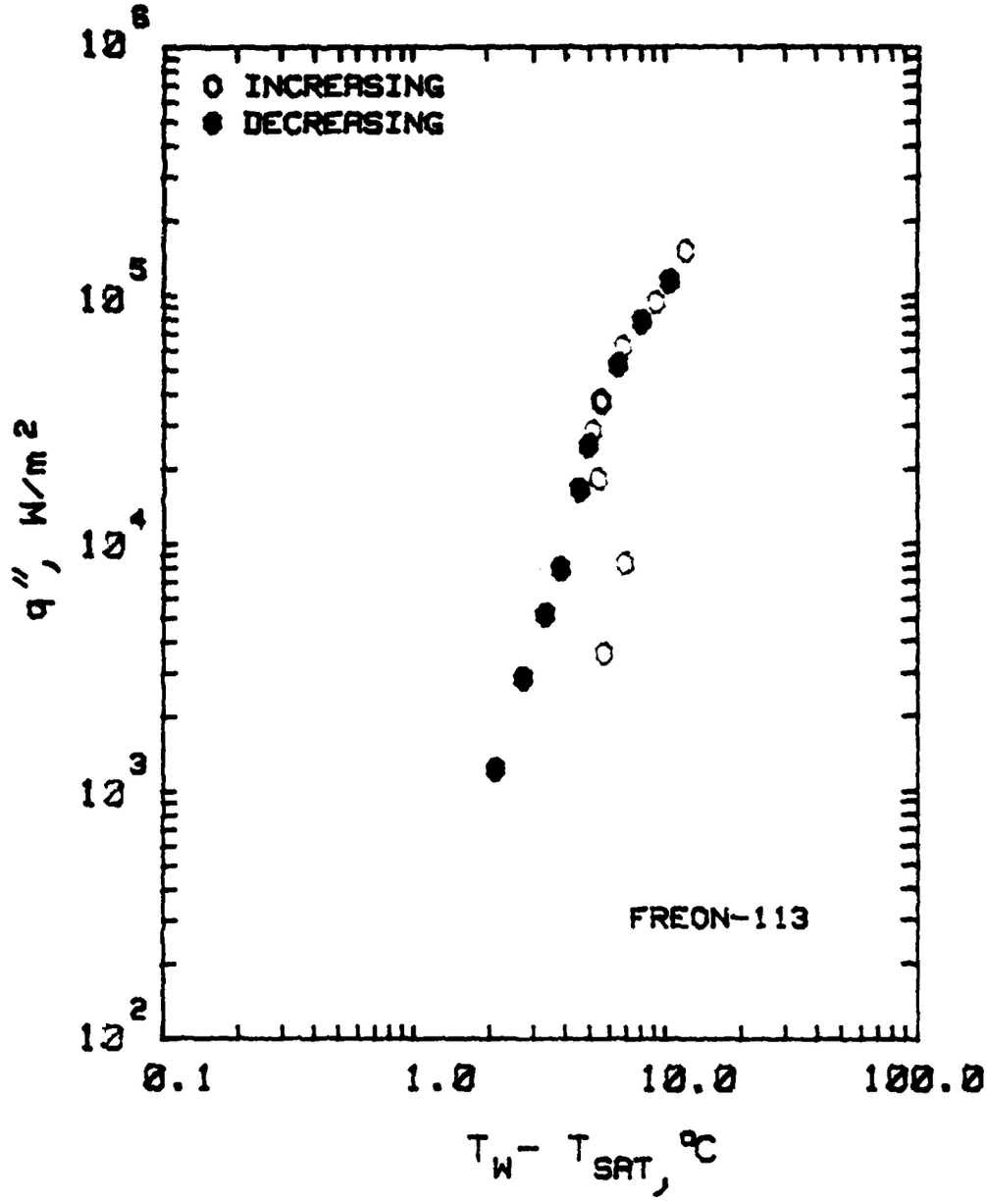

Figure 8. Procedure B: Standard Data

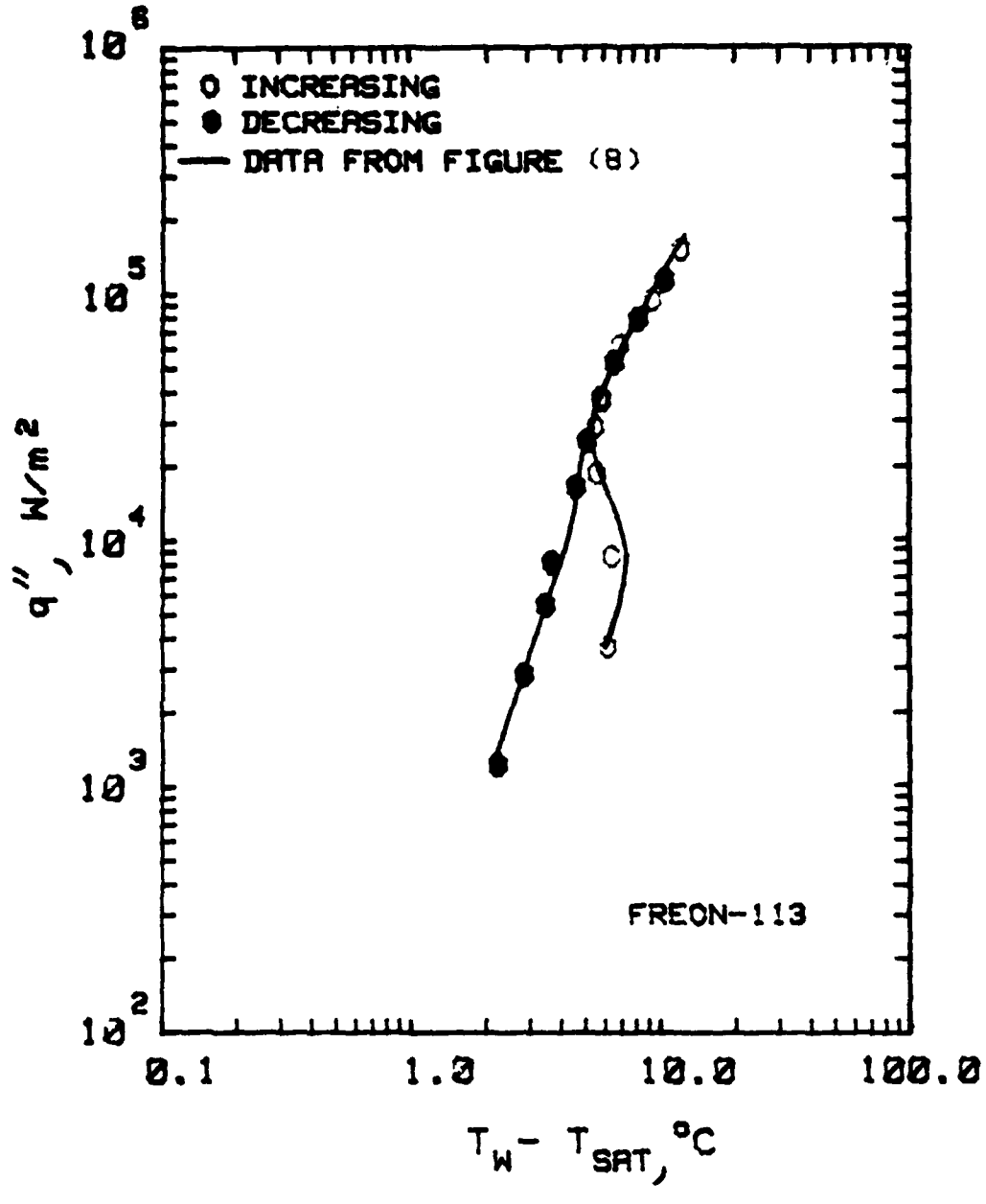

Figure 9. Reproducibility Test: Data Under Identical Conditions

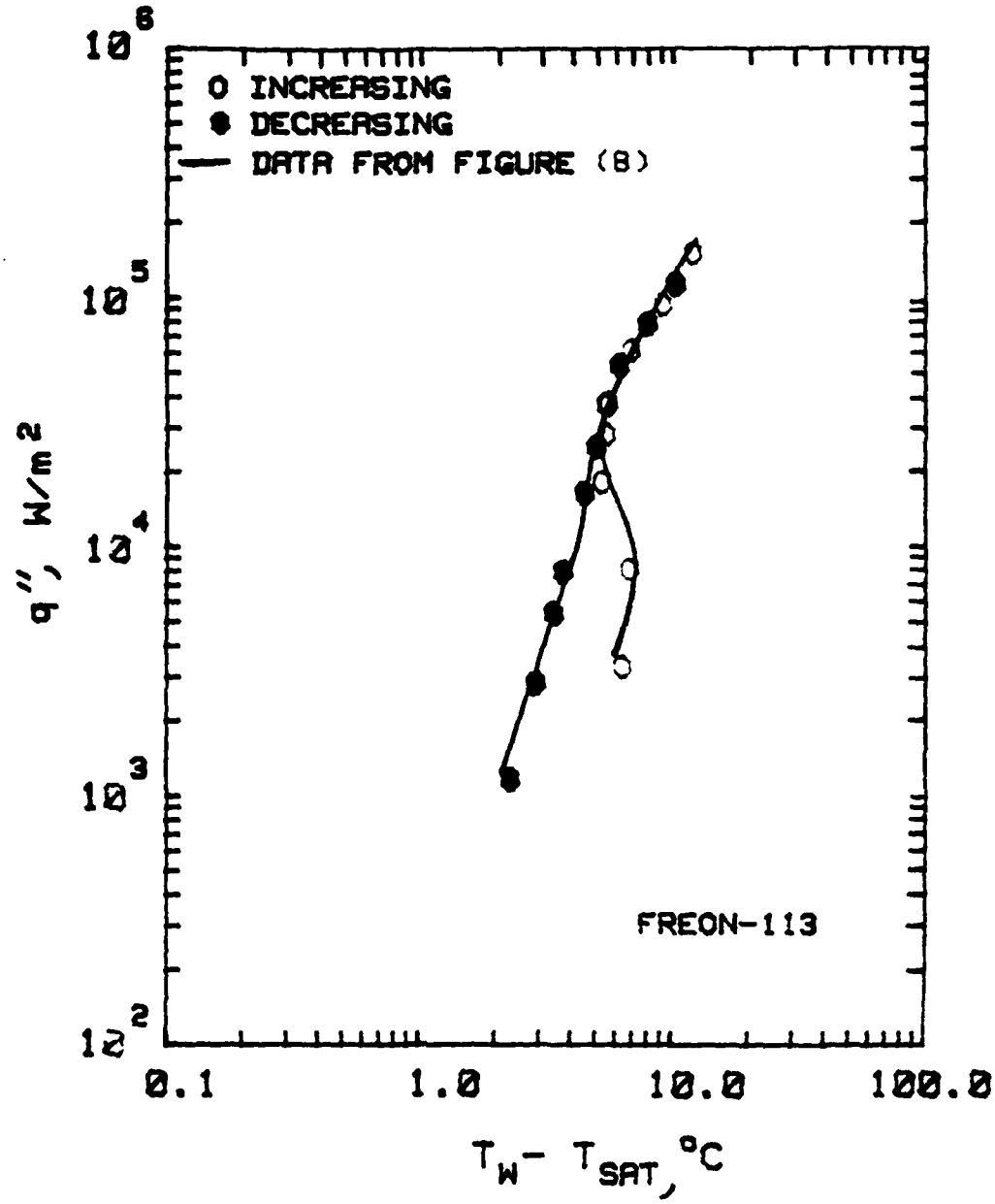

Figure 10. Reproducibility Test: Test Section Lowered to 38.1 mm

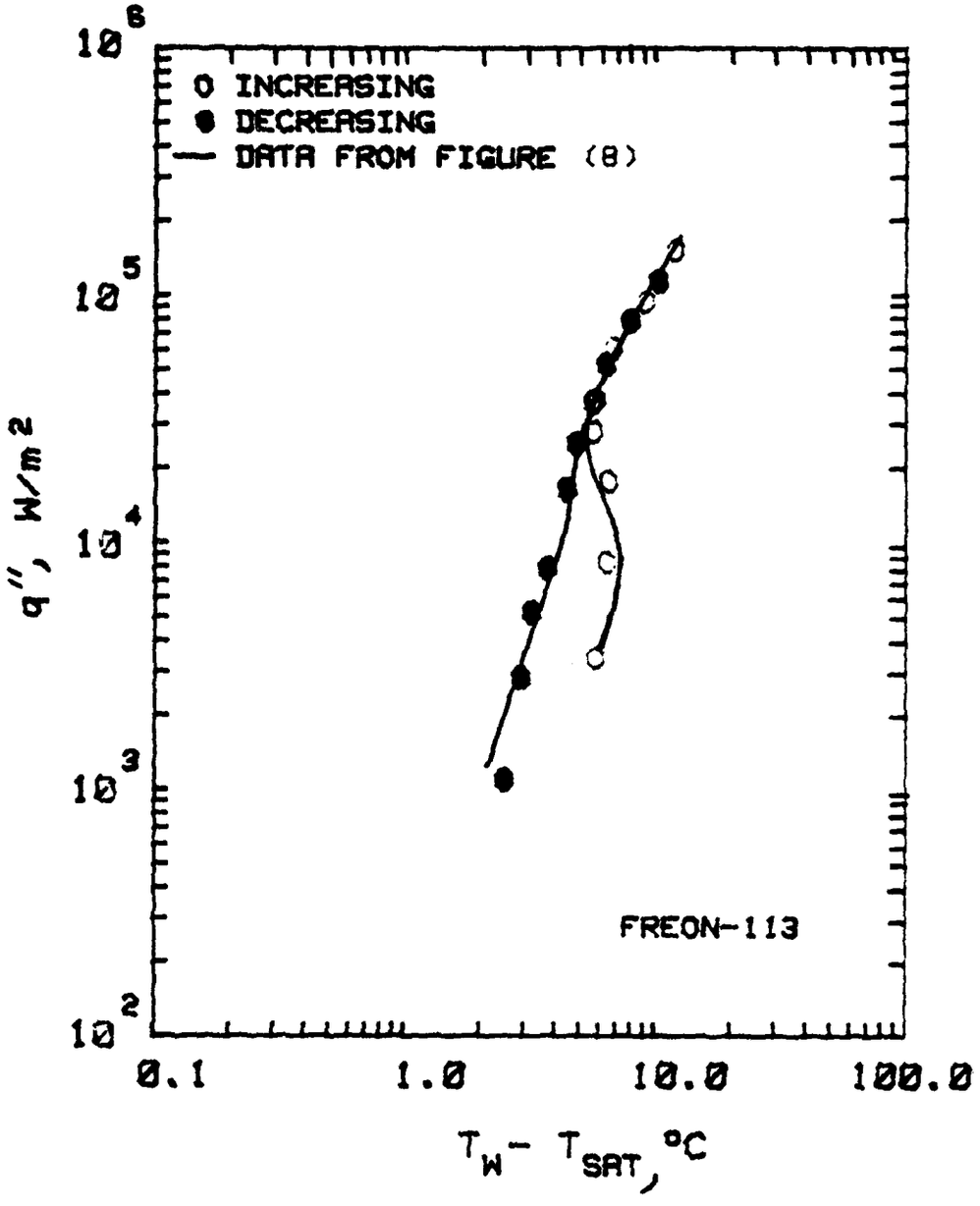

Figure 11. Reproducibility Test: Test Section Raised to 76.2 mm

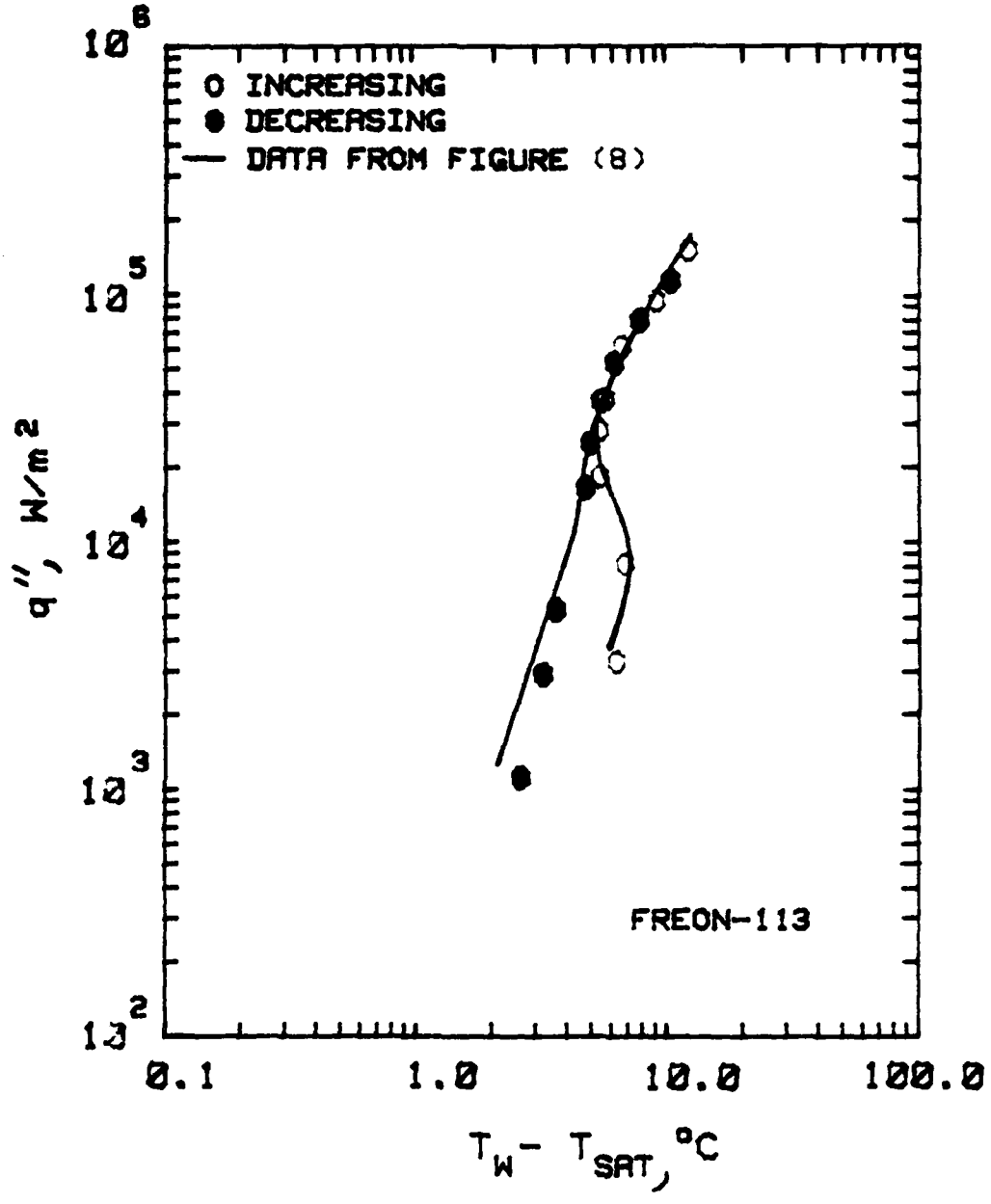

Figure 12. Reproducibility Test: Test Section Rotated 90°

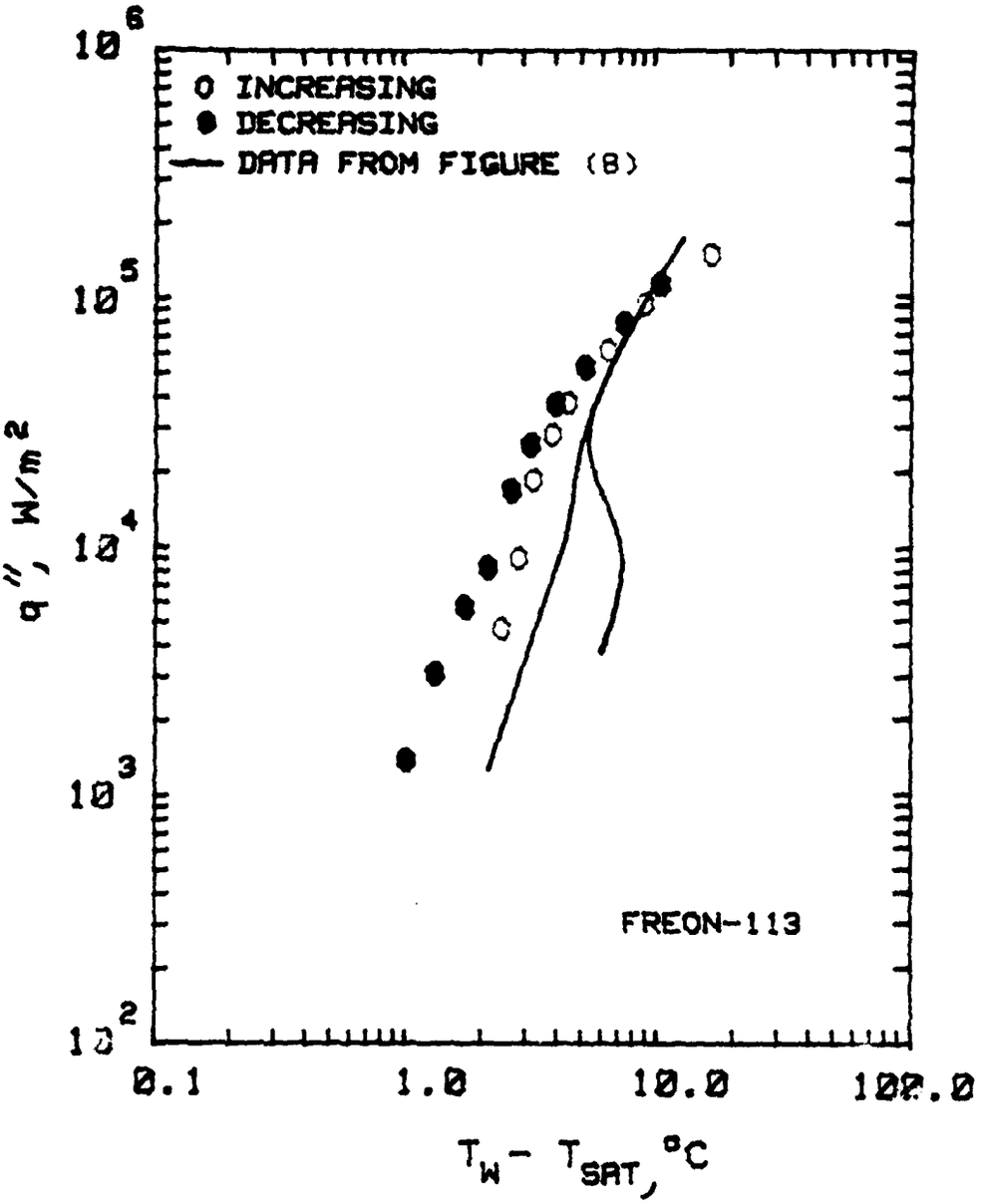

Figure 13. Application of 60°-60° Shroud

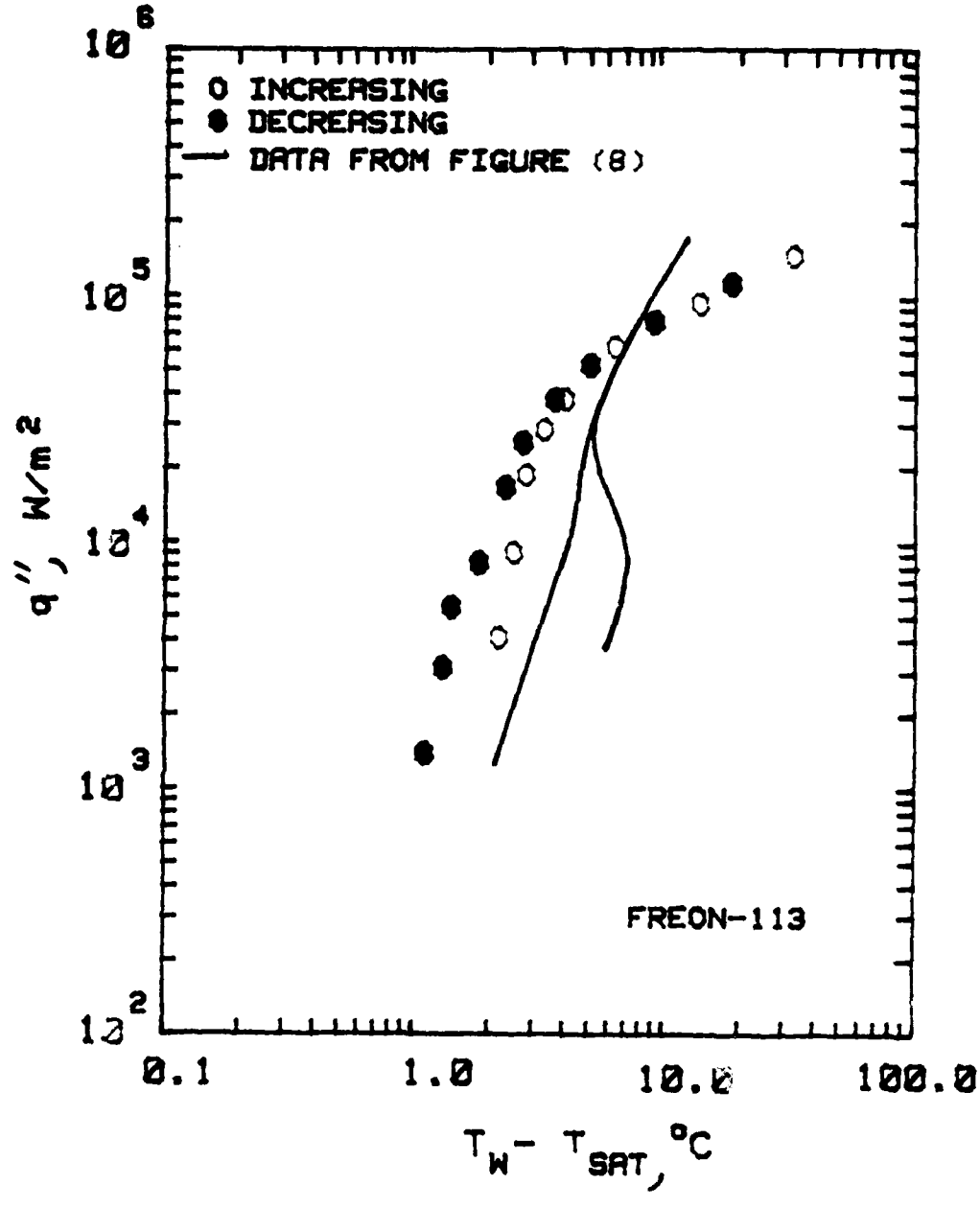

Figure 14. Application of 30°-30° Shroud

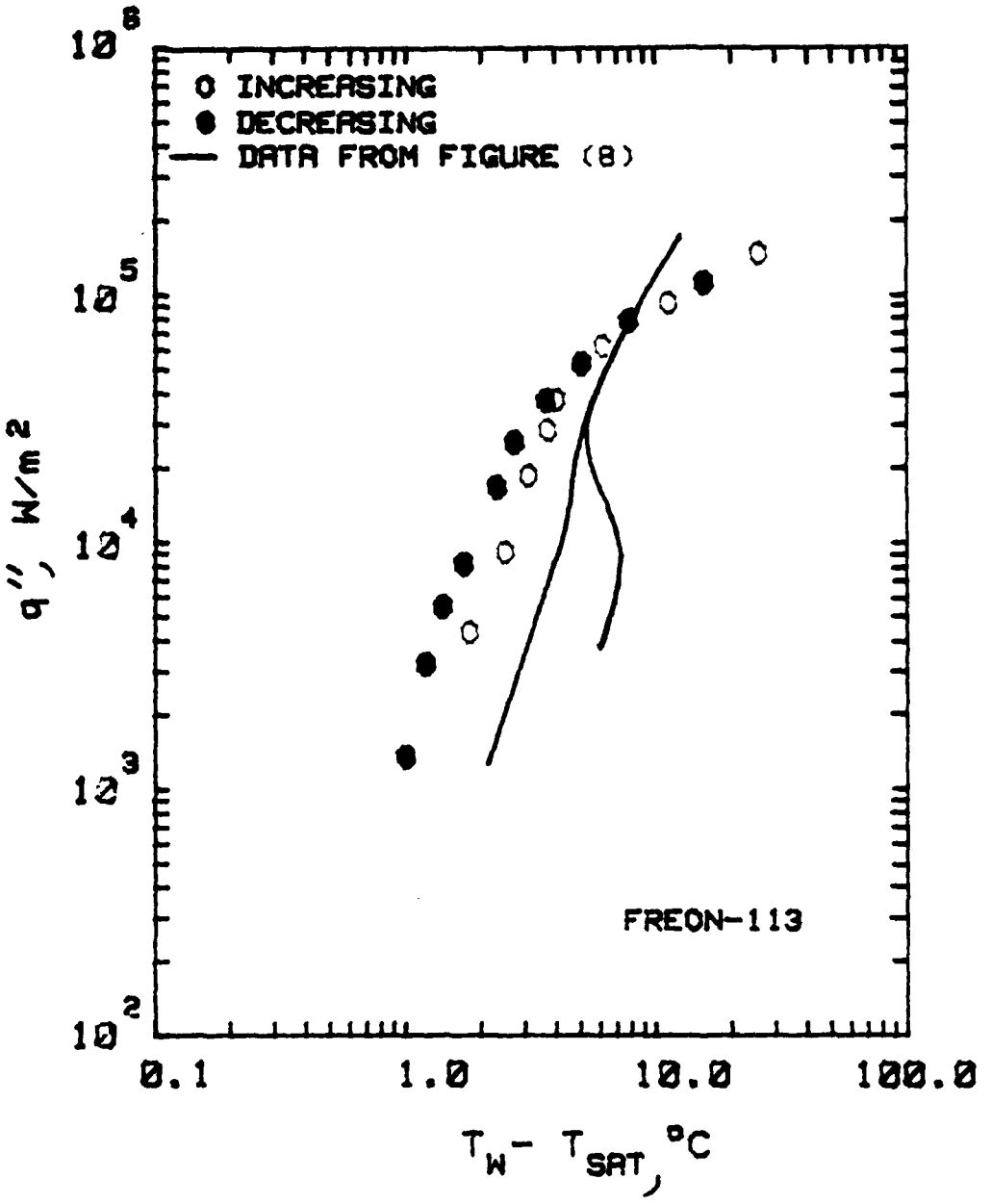

Figure 15. Application of 60°-30° Shroud

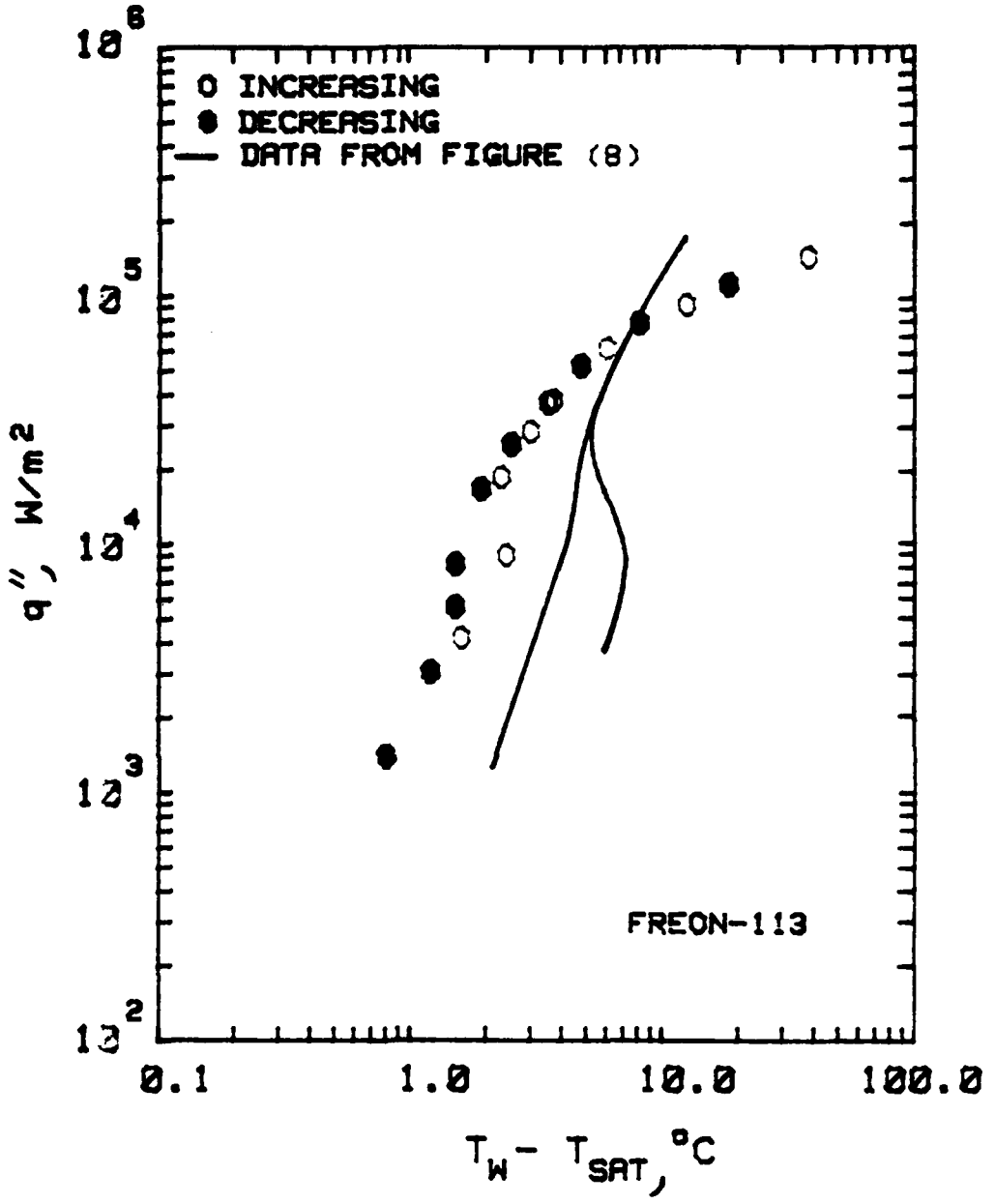

Figure 16. Application of 60°-8.5° Shroud

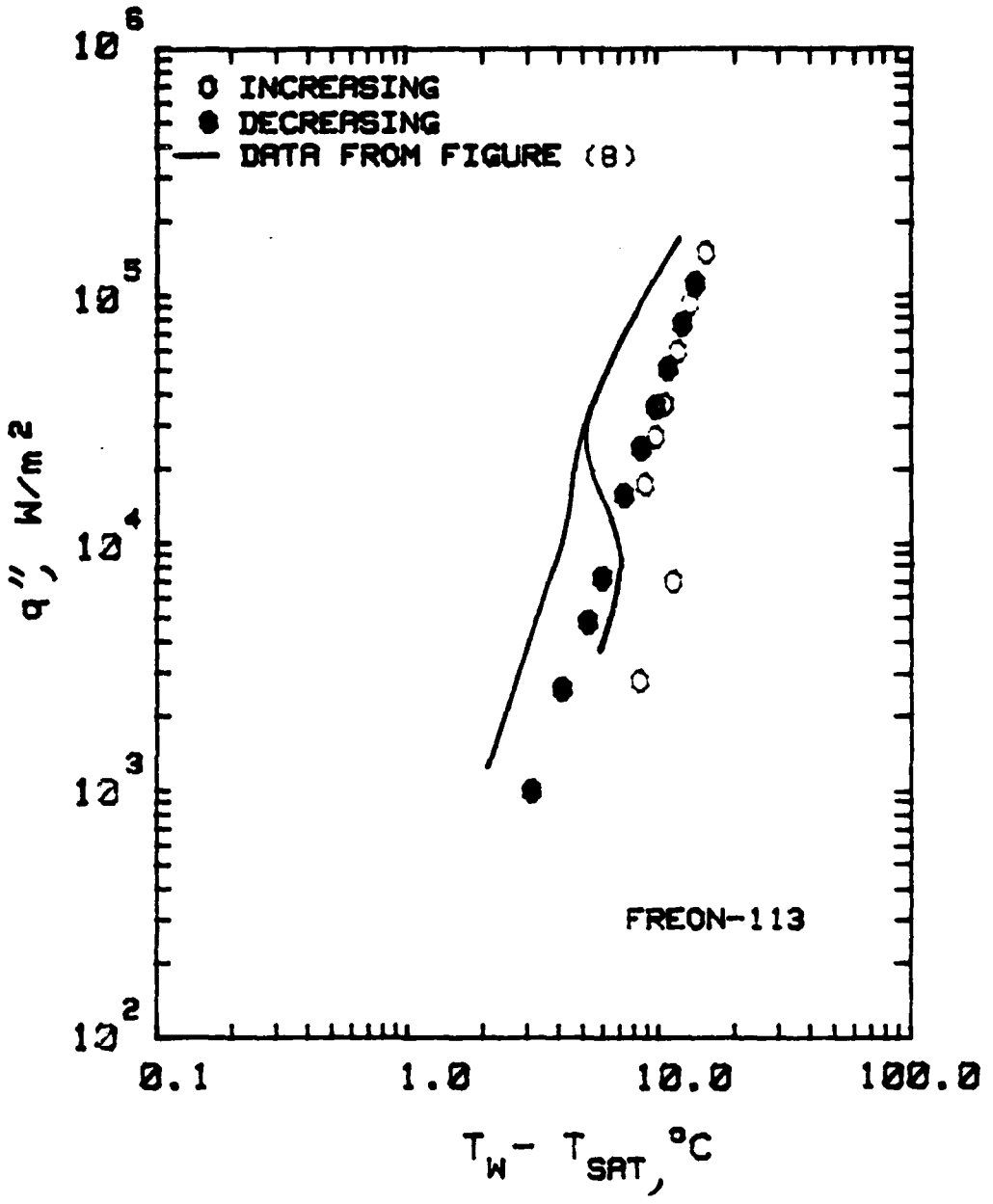

Figure 17. "T-caps" Removed, Straight Fins

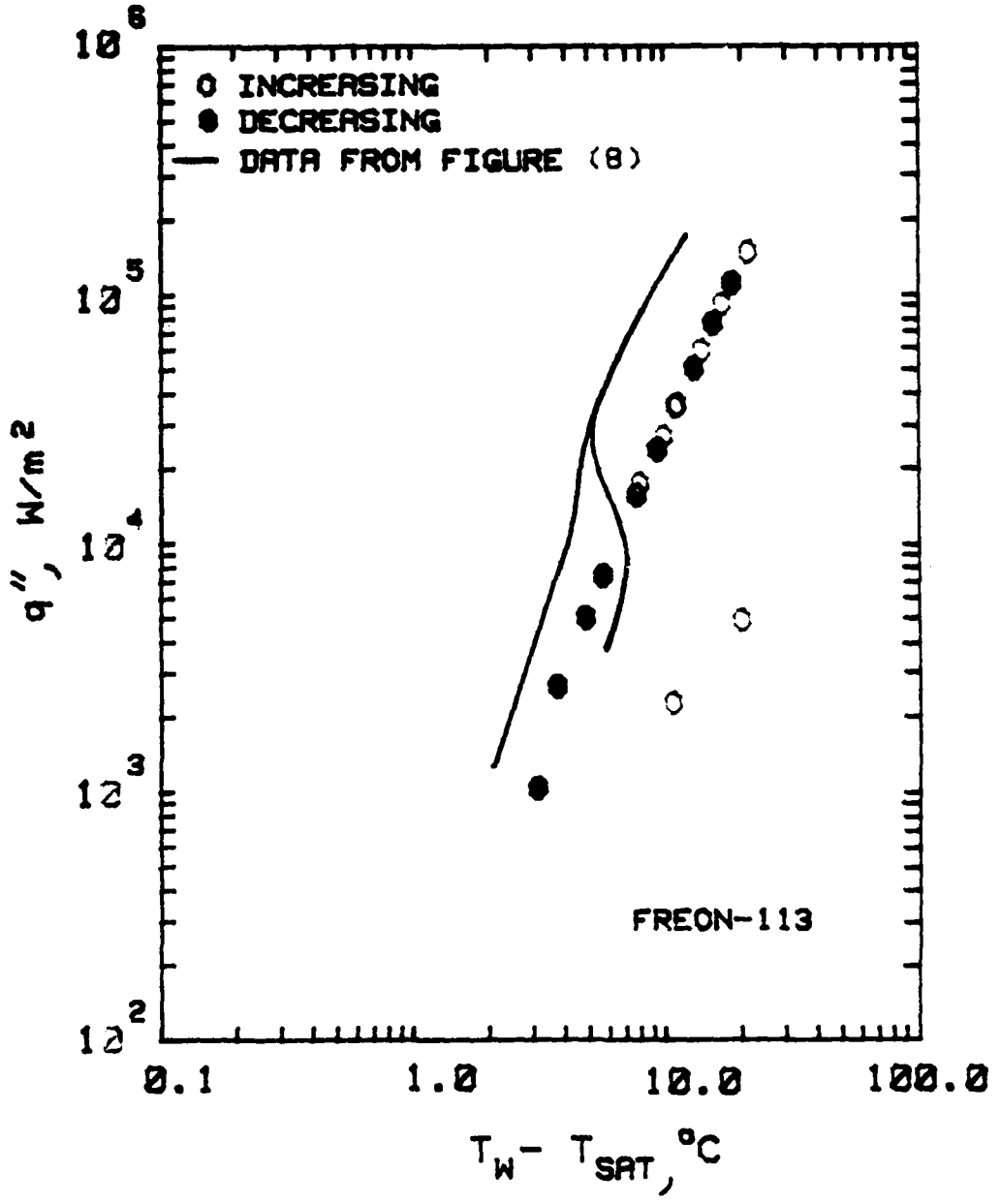

Figure 18. Fins Removed, Smooth Tube

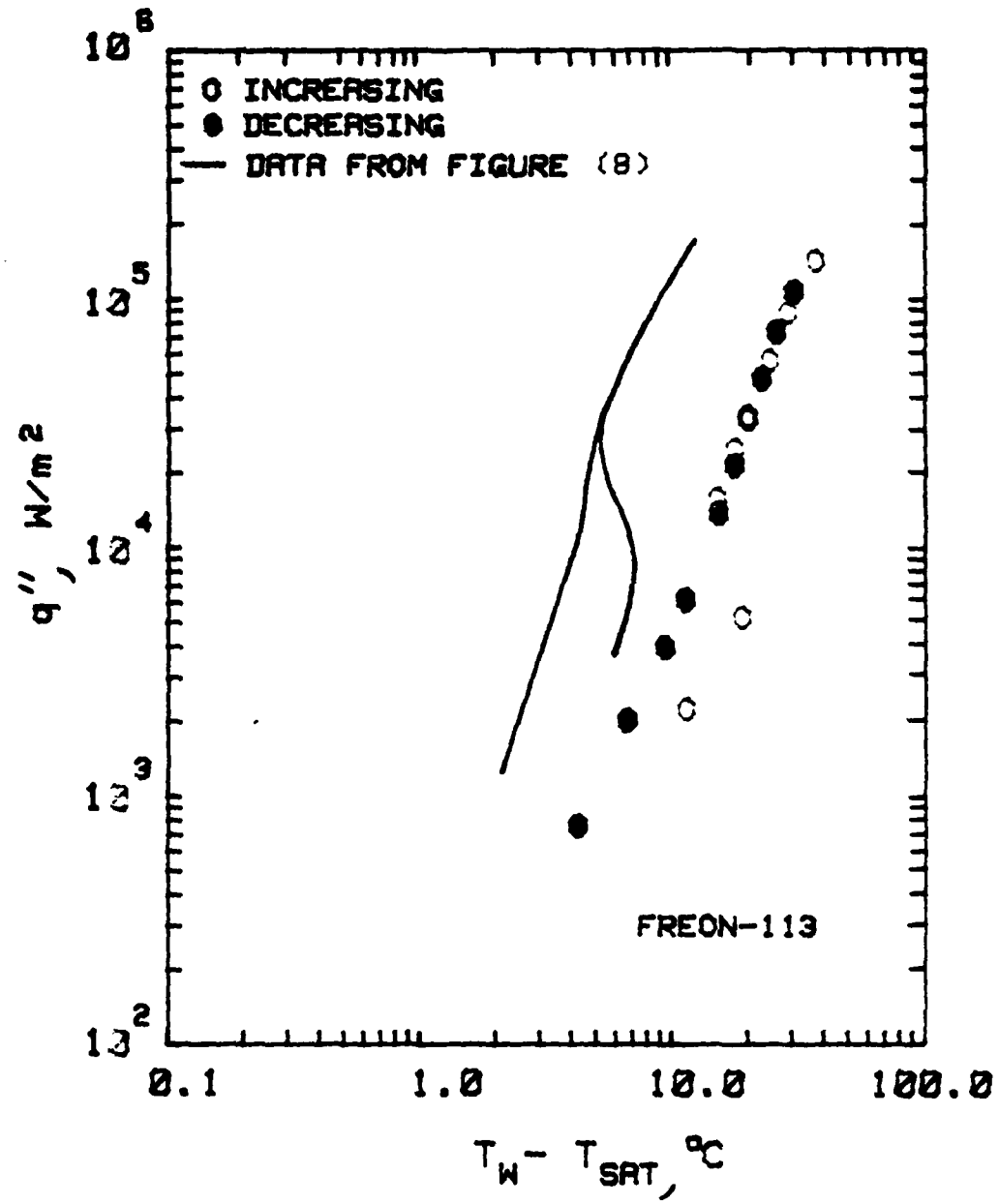

Figure 19. Mirror Polished Smooth Tube

LIST OF REFERENCES

1. Yilmaz, S., and Westwater, J., "Effect of Commercial Enhanced Surfaces on the Boiling Heat Transfer Curve," Advances in Enhanced Heat Transfer, p. 74, 1981.

2. Bergles, A., and Chyu, M., "Characteristics of Nucleate Pool Boiling from Porous Metallic Coatings," Advances in Enhanced Heat Transfer, p. 61, 1981.

3. Webb, R., "The Evolution of Enhanced Surface Geometries for Nucleate Boiling," Heat Transfer Engineering, v. 2, p. 61, 1981.

4. Bergles, A., and Chyu, M., "Characteristics of Nucleate Pool Boiling from Porous Metallic Coatings," Advances in Enhanced Heat Transfer, pp. 62-63, 1981.

5. Yilmaz, S., and Westwater, J., "Effect of Commercial Enhanced Surfaces on the Boiling Heat Transfer Curve," Advances in Enhanced Heat Transfer, pp. 80-91, 1981.

6. Marto, P., and Lepere, V., "Pool Boiling Heat Transfer from Enhanced Surfaces to Dielectric Fluids," Advances in Enhanced Heat Transfer, pp. 98-101, 1981.

7. Stephan, K., and Mitrovic, J., "Effects of Pore Diameters and System Pressure on Nucleate Pool Boiling Heat Transfer from Porous Surfaces," Advances in Enhanced Heat Transfer, pp. 131-146, 1981.

8. Ibid., pp. 139-140.

9. Bergles, A., and Chyu, M., "Characteristics of Nucleate Pool Boiling from Porous Metallic Coatings," Advances in Enhanced Heat Transfer, pp. 67-69, 1981.

10. Lepere, V., Nucleate Pool Boiling of High Dielectric Fluids from Enhanced Surfaces, M.S. Thesis, Naval Postgraduate School, Monterey, California, 1980.

11. Incropera, F.P., and DeWitt, D.P., Fundamentals of Heat Transfer, John Wiley and Sons, Inc., New York, N.Y., p. 447, 1981.

12. Ibid., p. 109.

13. Cornwell, K., Schüller, R., Einarsson, J., "The Influence of Diameter on Nucleate Pool Boiling Outside Tubes," Heat Transfer, v. 4, pp. 47-52, 1982.

14. ASHRAE Guide and Data Book, p. 261, p. 595, American Society of Heating, Refrigerating, and Air Conditioning Engineers, 1972.

INITIAL DISTRIBUTION LIST

		No. Copies
1.	Defense Technical Information Center Cameron Station Alexandria, Virginia 22314	2
2.	Library, Code 0142 Naval Postgraduate School Monterey, California 93940	2
3.	Department Chairman, Code 69 Department of Mechanical Engineering Naval Postgraduate School Monterey, California 93940	1
4.	Professor Paul J. Marto, Code 69Mx Department of Mechanical Engineering Naval Postgraduate School Monterey, California 93940	2
5.	Mr. Fred Weiler Wieland-America Incorporated Orange, New Jersey 07050	1
6.	Mr. Klaus Menze Wieland Werke AG WEST GERMANY	1
7.	LT B.G. Hernandez 701 Cabrillo Avenue Coronado, CA 92118	1

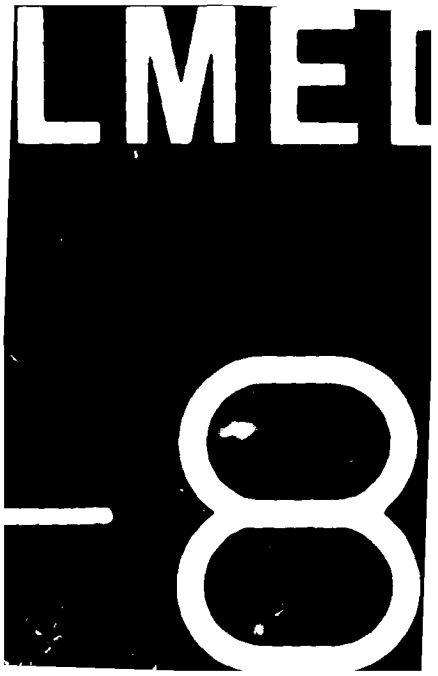
LMEL
8